



Published in final edited form as:

Nature. 2021 January ; 589(7842): 426–430. doi:10.1038/s41586-020-2991-4.

## A brainstem peptide system activated at birth protects postnatal breathing

Yingtang Shi<sup>1</sup>, Daniel S. Stornetta<sup>1</sup>, Robert J. Reklow<sup>2</sup>, Alisha Sahu<sup>1</sup>, Yvonne Wabara<sup>1</sup>, Ashley Nguyen<sup>1</sup>, Keyong Li<sup>1</sup>, Yong Zhang<sup>2</sup>, Edward Perez-Reyes<sup>1</sup>, Rachel A. Ross<sup>3,4</sup>, Bradford B. Lowell<sup>3</sup>, Ruth L. Stornetta<sup>1</sup>, Gregory D. Funk<sup>2</sup>, Patrice G. Guyenet<sup>1</sup>, Douglas A. Bayliss<sup>1</sup>

<sup>1</sup>Department of Pharmacology, University of Virginia, Charlottesville, Virginia, USA

<sup>2</sup>Department of Physiology, Women & Children's Health Research Institute, Neuroscience and Mental Health Institute, University of Alberta, Edmonton, Alberta, Canada

<sup>3</sup>Beth Israel Deaconess Medical Center, Harvard University, Boston, MA, USA

<sup>4</sup>McLean Hospital, Department of Psychiatry, Harvard Medical School, Belmont, MA, USA

### Abstract

Among numerous challenges encountered at the beginning of extrauterine life, the most celebrated is the first breath that initiates a life-sustaining motor activity 1. The neural systems that regulate breathing are fragile early in development, and how they adjust to support breathing at the time of birth is not well understood. Here, we identify a neuropeptide system that becomes activated immediately upon birth and supports breathing. Mice lacking pituitary adenylate cyclase-activating peptide (PACAP) selectively in retrotrapezoid nucleus (RTN) neurons displayed increased apneas and blunted CO<sub>2</sub>-stimulated breathing; re-expression of PACAP in RTN neurons corrected these breathing deficits. Deletion of the PACAP receptor, PAC1, from the pre-Bötzinger Complex (preBötC), an RTN target region responsible for respiratory rhythm generation, phenocopied breathing deficits observed with RTN deletion of PACAP, and suppressed PACAP-evoked respiratory stimulation in the preBötC. Notably, a striking postnatal burst of PACAP expression occurred in RTN neurons precisely at the time of birth, coinciding with exposure to the

---

Users may view, print, copy, and download text and data-mine the content in such documents, for the purposes of academic research, subject always to the full Conditions of use:[http://www.nature.com/authors/editorial\\_policies/license.html#terms](http://www.nature.com/authors/editorial_policies/license.html#terms)

**Corresponding author:** Correspondence to Douglas A. Bayliss: [dab3y@virginia.edu](mailto:dab3y@virginia.edu).

#### Author Contributions

YTS, GDF, PGG and DAB developed concepts and designed experiments. YTS developed shRNA constructs, produced lentivirus and contributed to all experiments (made viral injections, performed histochemistry, single cell molecular biology, plethysmography, RTN neuron electrophysiology dEMG recordings and *in vivo* PACAP injections). DSS performed histochemistry and data analysis. RJR and YZ performed *in vitro* rhythmic slice recordings, which were also analyzed by GDF. AS, YW, AN, and KYL analyzed histochemical and plethysmography data; KYL and YTS made adult mouse brainstem slices. EPR designed viral targeting constructs and subcloned shRNA. RAR and BBL provided mice with floxed PACAP alleles. RLS analyzed and interpreted histochemical data. YTS and DAB conceptualized and wrote the manuscript, and all authors edited the manuscript.

#### Competing Financial Interests statement

The authors declare that they have no competing financial interests.

#### Data and Reagent Availability.

The authors declare that all data supporting the findings of this study are available within the paper and its Supplementary Information files or from the corresponding author (D.A.B.); unique biological materials are available from the relevant authors upon reasonable requests.

external environment. Neonatal mice with deletion of PACAP in RTN neurons displayed increased apneas that were further exacerbated by changes in ambient temperature. Our findings demonstrate that well-timed PACAP expression by RTN neurons provides an important supplementary respiratory drive immediately after birth, and reveal key molecular components of a peptidergic neural circuit that supports breathing at a particularly vulnerable period in life.

Respiratory chemoreceptor neurons of the RTN provide a critical CO<sub>2</sub>/H<sup>+</sup>-modulated excitatory drive to the brainstem respiratory rhythm generator and pre-motor circuits that is primarily dependent on glutamate transmission<sup>2-4</sup>. Dysfunction of RTN neurons is implicated in congenital central hypoventilation syndrome (CCHS), a disorder caused by mutations in the *Phox2b* transcription factor and characterized by increased apneas and reduced respiratory CO<sub>2</sub> sensitivity<sup>52</sup>. All RTN chemoreceptor neurons express *Phox2b*, *Nmb*, and *PACAP*<sup>6</sup>. Interestingly, PACAP variants are associated with sudden infant death syndrome (SIDS)<sup>7</sup>, and PACAP-null mice display a SIDS-like phenotype, with apneas and blunted CO<sub>2</sub>-stimulated breathing<sup>8,9</sup>. We therefore examined a potential neuromodulatory role for PACAP in control of breathing by RTN neurons.

Mice with loxP sites at the *PACAP* gene were crossed to *Phox2b*-Cre mice (Fig. 1a)<sup>10,11</sup> and *PACAP* deletion was confirmed in *Phox2b*- and *Nmb*-expressing neurons in the RTN from *Phox2b::Cre;PACAP<sup>fl/fl</sup>* mice (Extended Data Fig. 1a,b). We assessed effects of PACAP deletion on respiration in these mice by whole body plethysmography, under hyperoxic conditions to minimize influence of peripheral chemoreceptors. CO<sub>2</sub>-stimulated breathing was depressed in Cre-positive PACAP<sup>fl/fl</sup> mice, relative to Cre-negative control littermates (by ~25% at 8% CO<sub>2</sub>, Fig. 1b), largely due to a reduced effect of CO<sub>2</sub> on breathing frequency (Extended Data Fig. 1c,d). There was no genotype-dependent difference in hypoxia-stimulated breathing (10% FiO<sub>2</sub>; Extended Data Fig. 1e), which is not driven by RTN neurons<sup>2</sup>. In addition, these mice displayed a 4-fold higher incidence of spontaneous apneas (Fig. 1c).

We employed a series of complementary lentiviral injection/expression strategies to target RTN neurons more selectively and to manipulate PACAP expression more acutely. For this, lentiviral constructs expressing Cre or PACAP, driven by the *Phox2b*-responsive PRSx8 promoter, were injected, respectively, into the RTN of PACAP<sup>fl/fl</sup> mice (knockout) or Cre-positive PACAP<sup>fl/fl</sup> mice (rescue) (Fig. 1a, Extended Data Fig. 2a)<sup>12-14</sup>. This approach provided high transduction efficiency and specificity: at 4 weeks following injection, ~40%–80% of *Nmb*<sup>+</sup> RTN neurons were virally-transduced (mCherry<sup>+</sup>) and ~87%–100% of mCherry<sup>+</sup> cells contained the specific RTN neuron marker, *Nmb* (Extended Data Fig. 2b,c)<sup>6</sup>, with no difference between experimental and control virus. This preferential transduction of *Nmb*<sup>+</sup> cells indicates that our injections largely avoided nearby *Phox2b*-expressing C1 neurons<sup>6</sup>, which rarely express *PACAP* at this rostrocaudal level (Extended Data Fig. 2d–f). In PACAP<sup>fl/fl</sup> mice injected with virus expressing Cre-mCherry, but not mCherry alone, PACAP expression was undetectable in most infected RTN neurons (Extended Data Fig. 2g). Correspondingly, CO<sub>2</sub>-stimulated ventilation (V<sub>E</sub>) was decreased from the pre-injection control (by ~50%), via effects on both frequency (fR) and tidal volume (V<sub>T</sub>), and apnea frequency was increased ~4-fold from pre-injection control (Fig. 1d, Extended Data Fig. 2h–

j). Conversely, viral-mediated re-expression of PACAP in RTN neurons of *Phox2b::Cre;PACAP<sup>fl/fl</sup>* mice restored CO<sub>2</sub>-stimulated breathing and rescued apnea frequency to levels observed in Cre-negative PACAP<sup>fl/fl</sup> littermates, an effect not seen in mice injected with control virus (Extended Data Fig. 2b, Fig. 1e).

We leveraged this lentiviral approach to deliver control and PACAP shRNA lentivirus to the RTN region in *Phox2b::GFP* mice with wild type PACAP alleles (Fig. 1f, Extended Data Fig. 3a). For both PACAP and scrambled shRNA lentivirus, viral transduction was again efficient and specific (~34–87% of RTN neurons were transduced, and ~95–98% of transduced cells were RTN neurons; Extended Data Fig. 3b). We confirmed depletion of *PACAP* transcripts in RTN neurons transduced with PACAP shRNA, whereas *PACAP* expression was unaffected in nearby uninfected RTN neurons and unchanged in both infected and uninfected RTN neurons from mice injected with control lentivirus (Fig. 1f, Extended Data Fig. 3c,e). Moreover, there was no effect of either construct on expression of VGlut2 (*Slc17a6*), the vesicular transporter required for glutamate-mediated respiratory effects of RTN<sup>3,4</sup> (Extended Data Fig. 3d,e). The ventilatory response to CO<sub>2</sub> was unaffected by control shRNA but sharply reduced by PACAP shRNA (~40%), reflecting blunted CO<sub>2</sub>-induced increases in both fR and V<sub>T</sub> (Fig. 1g, Extended Data Fig. 3f,g). Again, *PACAP* depletion in RTN neurons had no effect on hypoxia-stimulated breathing (Extended Data Fig. 3h) but caused a ~3-fold increase in apneas (Fig. 1g). These findings indicate that PACAP supports respiratory drive from CO<sub>2</sub>/H<sup>+</sup>-sensitive RTN neurons.

The blunted CO<sub>2</sub>-stimulated breathing in mice following *PACAP* depletion in RTN could reflect reduced activation of RTN neurons, or altered neuropeptide signaling to downstream respiratory effector neurons. Therefore, we first tested whether *PACAP* depletion affected the CO<sub>2</sub>/H<sup>+</sup>-sensitivity of RTN neurons, *in vitro* and *in vivo*. The effect of pH on RTN neuron firing in neonatal mouse brainstem slices<sup>12,14</sup> was unaffected by Cre-mediated deletion of PACAP (Extended Data Fig. 4a,b) and, in a subset of neurons assayed by multiplex single cell qPCR following recording, we found no effect on expression of the two putative RTN proton sensors (*Gpr4*, *Kcnk5*; Extended Data Fig. 4c)<sup>2,14</sup>. *In vivo*, there was no difference in CO<sub>2</sub>-induced Fos expression in RTN neurons, a surrogate for neuronal activation, after either Cre-mediated PACAP deletion (Extended Data Fig. 2k) or shRNA-mediated knockdown of *PACAP* (Extended Data Fig. 4d)<sup>12</sup>. This indicates that RTN neurons retain the ability to respond to CO<sub>2</sub>/H<sup>+</sup> after *PACAP* depletion and suggests that local PACAP autocrine/paracrine signaling is not critical for normal RTN activation by CO<sub>2</sub>. Indeed, we found only sparse expression of *PAC1*, the PACAP receptor, in RTN neurons (<5%, Extended Data Fig. 4e).

We next examined whether PACAP contributions to CO<sub>2</sub>-stimulated breathing are mediated downstream of CO<sub>2</sub>/H<sup>+</sup>-activated RTN neurons, e.g., by PAC1-expressing RTN neuronal targets that regulate breathing. RTN neurons project to respiratory-related brainstem areas (Extended Data Fig. 4g)<sup>2</sup>, and mCherry<sup>+</sup> fibers from viral-infected RTN neurons were evident around somatostatin (*Sst*)-expressing neurons in the preBötC (Extended Data Fig. 4h), a region that contains the core circuitry for respiratory rhythm generation<sup>1,15</sup>. In the preBötC, *PAC1* expression and CO<sub>2</sub>-evoked Fos induction were observed in neurons and, less frequently, in astrocytes (Extended Data Fig. 4i). In neurons, CO<sub>2</sub>-induced Fos

expression was found in *PAC1*-containing excitatory and inhibitory neurons, which function interdependently to regulate breathing rhythm<sup>16</sup>, and also in cells that did not express detectable levels of *PAC1* (Extended Data Fig. 4i). Importantly, regardless of cell type, CO<sub>2</sub>-evoked Fos expression in the preBötC region was strongly reduced in mice after either shRNA- or Cre-mediated *PACAP* depletion in RTN neurons (Fig. 2a,b, Extended Data Fig. 4f). These data suggest that respiratory effects of RTN-expressed PACAP are mediated, in part, by PAC1 receptor-expressing neurons within the preBötC.

To test whether the preBötC is a relevant site for respiratory effects of PACAP, we made pressure microinjections of PACAP directly into the preBötC of anesthetized mice while recording diaphragmatic EMG (dEMG) as a measure of central respiratory output (Fig. 2c,d). PACAP increased both the frequency and amplitude of dEMG bursts (Fig. 2d,f, Extended Data Fig. 5a). These effects were not mimicked by vehicle injections and were dependent on pipette location relative to the preBötC (Fig. 2e,f, Extended Data Fig. 5a,b). In addition, microinjection of PACAP into the preBötC region of a rhythmic neonatal slice preparation, in which bursting respiratory motor nerve activity denotes fictive respiratory drive<sup>1</sup>, yielded concentration-dependent increases in respiratory frequency that were not different across a range of neonatal time points (P0-P10) (Fig. 2g,h, Extended Data Fig. 5e-g). As in the adult, *PAC1*-expressing cells overlapped and intermingled with *Sst*-expressing neurons in the perinatal preBötC, whereas VPAC1 and VPAC2 receptor transcripts (also activated by PACAP<sup>17</sup>) were undetectable in preBötC neurons at any age examined (Extended Data Fig. 5h,i).

We used shRNA-mediated knockdown to test whether PAC1 in preBötC neurons contributes to respiratory effects of PACAP (Fig. 3a). PAC1 is expressed in multiple cell types in the preBötC (Extended Data Fig. 4i), which is a molecularly and functionally heterogeneous group of neurons<sup>1</sup>. Therefore, viral shRNA constructs and mCherry were driven by separate, non-selective promoters (H1, EF1 $\alpha$ ). Four weeks after bilateral virus injections, *PAC1* expression was clearly reduced in PAC1 shRNA-expressing preBötC neurons (Fig. 3a). Infected neurons covered a variable amount of the preBötC in individual mice, but there was no difference in the average coverage for PAC1 and control shRNAs (Extended Data Fig. 6a-c). Following unilateral shRNA knockdown of *PAC1*, the stimulatory effects of ipsilateral PACAP injection on respiratory output (dEMG) were reduced at preBötC sites where DL-homocysteic acid (DLH) remained effective (Fig. 3b,d,e, Extended Data Fig. 5c); by contrast, respiratory effects of PACAP microinjections were preserved in mice transduced with control shRNA (Fig. 3c,e) or in which the PAC1 shRNA virus injection was mistargeted (Extended Data Fig. 5d).

After CO<sub>2</sub> exposure, the number of Fos-expressing cells in the preBötC of *PAC1*-depleted mice was reduced by ~74% relative to CO<sub>2</sub>-exposed mice infected with control shRNA (Fig. 3f,g), to levels comparable to those observed following *PACAP* deletion in RTN or in control mice not exposed to CO<sub>2</sub> (confidence interval in Fig. 3g). *PAC1* depletion in the preBötC was associated with blunted CO<sub>2</sub>-stimulated breathing (~24%), in this case due to diminished effects on fR (Fig. 3h, Extended Data Fig. 6d,e), and again with no effect on hypoxia-stimulated breathing (Extended Data Fig. 6f). *PAC1* depletion in the preBötC also

increased apnea frequency (~2-fold; Fig. 3h), further phenocopying effects of *PACAP* depletion in RTN neurons.

Global deletion of *PACAP* in mice is associated with cardiorespiratory disturbances and greater susceptibility to death in the early postnatal period<sup>8,9,18</sup>. As noted, *PAC1* receptor expression in the preBötC approximated adult levels throughout development (Extended Data Fig. 5h). By contrast, *PACAP* transcripts appeared at low levels in RTN neurons in the late embryonic period up to e19.5, increased sharply in the days immediately after birth (P0-P3), and then gradually diminished through the early postnatal period and into adulthood (Fig. 4a,b, Extended Data Fig. 7a,b). This striking developmental expression pattern was not observed for other transcripts in RTN neurons (Extended Data Fig. 7c), or for *PACAP* in the NTS or in nearby *TH*-expressing C1 neurons (Extended Data Fig. 7d).

We tested whether this prominent increase in RTN neuronal *PACAP* expression, precisely between e19.5 and P0, reflected a well-timed gene regulatory program or was related to changes that occur in association with birth. To this end, we injected timed-mated pregnant dams with the antiprogesterone mifepristone (RU486) to precipitate pre-term birth at different embryonic time points (e17.5-e19.5)<sup>19</sup>. The pre-term pups were retrieved and processed for *in situ* hybridization or sc-qPCR within 10–60 min after birth and, in some cases, before the mother had extracted the pup from the amniotic sac (*en caula*) (Fig. 4c). Remarkably, and unlike their embryonic counterparts *in utero*, *PACAP* expression was already apparent in RTN neurons from pre-term mice that were delivered as early as e17.5 (Fig. 4d,e, Extended Data Fig. 8a). This rapid increase of *PACAP* expression after birth was not observed in mice that were retrieved from within the amniotic sac (Fig. 4d,e, Extended Data Fig. 8a), suggesting that *PACAP* upregulation may be stimulated by exposure to the ambient environment, and it became apparent within minutes after birth (Fig. 4f,g). Again, these early postnatal changes in *PACAP* expression were not observed for other genes examined in RTN neurons (Extended Data Fig. 8b). Thus, a striking and selective burst of *PACAP* expression occurs in RTN neurons at the time of birth, upon initiation of air breathing.

Finally, we tested whether *PACAP* in *Phox2b*-expressing neurons also contributes to breathing in neonatal mice (Fig. 4h). Indeed, CO<sub>2</sub>-stimulated ventilation was severely blunted (by >50%) in *Phox2b::Cre;PACAP<sup>fl/fl</sup>* mouse pups throughout the early neonatal period (P2-P12), by comparison to Cre-negative *PACAP<sup>fl/fl</sup>* littermates, via effects on both tidal volume and breathing frequency (Fig. 4i, Extended Data Fig. 9a,b,d). In addition, neonatal *Phox2b::Cre;PACAP<sup>fl/fl</sup>* mouse pups showed a ~3-fold greater incidence of apneic episodes versus control littermates under hyperoxic conditions (Fig. 4j, Extended Data Fig. 9c). We examined apnea frequency in two further cohorts of conditional knockout pups under normoxic conditions, in which peripheral chemoreceptor inputs could offset loss of RTN drive<sup>2</sup>; we additionally paired that with acute thermal stressors that can cause disordered breathing in neonates with underdeveloped thermoregulatory systems<sup>20</sup>, as observed previously in *PACAP*-deleted mouse pups (cold)<sup>8,21</sup> or associated with SIDS in human infants (warm)<sup>22</sup>. Apnea frequency remained ~3-fold higher in Cre-positive *PACAP<sup>fl/fl</sup>* mouse pups, relative to Cre-negative littermates in normoxia under thermoneutral conditions (30°C)<sup>20</sup>. Moreover, while exposure to either cooler or warmer temperatures increased apnea frequency in both Cre-negative and Cre-positive mice, the incidence of

apnea remained ~3-fold higher in Cre-positive pups, yielding a much larger increase in the absolute number of apneas (Fig. 4j, Extended Data Fig. 9e). Thus, PACAP in Phox2b-expressing neurons is protective of respiration in neonatal mice, including during breathing disturbances provoked by acute thermal stress.

Collectively, this work identifies a PACAP/PAC1-based neuropeptide brainstem microcircuit within a specific respiratory chemosensory network that reinforces breathing control systems, and which activates during the critical neonatal period when an otherwise immature and fragile respiratory control system transitions from producing periodic fetal breathing movements to continuous air-breathing. Even under normal conditions, neonates display blunted CO<sub>2</sub>-stimulated breathing and disordered breathing<sup>23</sup>, and dysfunction in homeostatic chemosensory systems is often implicated in early childhood breathing disturbances (e.g., CCHS, apnea of prematurity, SIDS)<sup>23</sup>. SIDS is a leading cause of postnatal death, but remains a syndrome without a positive diagnosis<sup>24,25</sup>. A prevailing triple-threat hypothesis holds that some undefined combination of genetic predisposition, environmental stressor (e.g., thermal stress), and critical period converge with lethal consequences<sup>22,25,26</sup>. Among possible predisposing factors, genetic variants in *PACAP* and *PAC1* have been associated with SIDS, albeit inconclusively<sup>7,27</sup>; brainstem abnormalities in PACAP and PAC1 have been observed in postmortem specimens from human SIDS infants<sup>28</sup>; and neonatal mice with global genetic deletion of *PACAP* display blunted CO<sub>2</sub>- and hypoxia-induced ventilatory stimulation together with a SIDS-like phenotype<sup>8,9,18</sup>. Our data define CO<sub>2</sub>-sensitive RTN neurons as a relevant neural substrate in which *PACAP* expression is upregulated precisely at birth, a critical period for regulating breathing; the normal developmental decrease of this neuropeptide system, or its pathological disruption, may provide predisposing conditions that increase susceptibility to the stress-induced apneas and blunted CO<sub>2</sub>-stimulated homeostatic responses implicated in SIDS and other neonatal breathing disturbances.

## Materials and Methods

Experiments were performed on mice of either sex, following procedures adhering to National Institutes of Health Animal Care and Use Guidelines and approved by the Animal Care and Use Committee of the University of Virginia, or in accordance with the guidelines of the Canadian Council on Animal Care and approved by the University of Alberta Animal Ethics Committee. Mice were housed in 12:12 dark:light conditions, with temperature ~22–24°C and ~40% relative humidity (30–70%). These studies used multiple different mouse lines: FVB and C57BL/6 mice were obtained from Jackson Labs; a Phox2b::GFP BAC transgenic mouse line (Jx99) was developed by the GENSAT project and characterized previously<sup>30</sup>; a previously described Phox2b::Cre BAC transgenic mouse line<sup>11</sup> was obtained from Jackson Labs (Stock #016223); and a mouse line with targeted insertion of loxP sites surrounding exon 2 of *Adcyap1* (the PACAP gene) was kindly provided by Drs. Rachel Ross and Brad Lowell (Beth Israel Deaconess Medical Center, Boston, MA)<sup>10</sup>. We crossed mice with floxed PACAP alleles to Phox2b-Cre mice<sup>10,11</sup> which yielded *PACAP*<sup>fl/fl</sup> mice that were Cre-positive (47%) and Cre-negative (53%) at near Mendelian proportions (220 pups; 7 breedings, one male and two females each). Experiments were performed on adult mice (8–15 weeks old), unless otherwise indicated. Mice were randomly assigned to

experimental/control group, with sample size chosen based on existing literature and previous experience with similar studies.

### Brainstem slice preparation

For cellular electrophysiology and single neuron harvest from neonatal and adult Jx99 mice, transverse brainstem slices were prepared as described previously<sup>6,12,31</sup>. For neonates, mice were anesthetized by hypothermia (<P5) or with ketamine and xylazine (375 mg/kg and 25 mg/kg, i.m.) and rapidly decapitated; brainstems were immediately removed and slices (300  $\mu$ m) cut with a vibrating microslicer (DTK Zero 1; Ted Pella, Redding, CA) in an ice-cold, sucrose-substituted Ringer's solution containing the following (in mM): 260 sucrose, 3 KCl, 5 MgCl<sub>2</sub>, 1 CaCl<sub>2</sub>, 1.25 NaH<sub>2</sub>PO<sub>4</sub>, 26 NaHCO<sub>3</sub>, 10 glucose, and 1 kynurenic acid. Slices were incubated for 30 min at 37°C, and subsequently at room temperature, in normal Ringer's solution containing the following (in mM): 130 NaCl, 3 KCl, 2 MgCl<sub>2</sub>, 2 CaCl<sub>2</sub>, 1.25 NaH<sub>2</sub>PO<sub>4</sub>, 26 NaHCO<sub>3</sub>, and 10 glucose. The cutting and incubation solutions were bubbled with 95% O<sub>2</sub> and 5% CO<sub>2</sub>. Adult mice (from 50-day old to 200-day old) were deeply anesthetized by intraperitoneal injection of ketamine (as above), and perfused transcardially with 25–30 ml of ice-cold NMDG aCSF (in mM: 93 NMDG, 2.5 KCl, 1.2 NaH<sub>2</sub>PO<sub>4</sub>, 30 NaHCO<sub>3</sub>, 20 HEPES, 25 glucose, 5 Na-ascorbate, 2 thiourea, 3 Na-pyruvate, 12 N-acetyl-L-cysteine, 10 MgSO<sub>4</sub>, 0.5 CaCl<sub>2</sub>, pH was adjusted to 7.3–7.4 with 10N HCl) saturated with 95% O<sub>2</sub>/5% CO<sub>2</sub>. The mice were rapidly decapitated, and the heads were submerged in ice-cold NMDG aCSF, bubbled with 95% O<sub>2</sub>/5% CO<sub>2</sub>, and the brainstems removed and cut in the coronal plane (150  $\mu$ m) with the vibrating microslicer in the same solution. After a brief recovery period (12 min in NMDG aCSF at 32–34 °C) the slices were transferred into HEPES holding aCSF (in mM: 92 NaCl, 2.5 KCl, 1.2 NaH<sub>2</sub>PO<sub>4</sub>, 30 NaHCO<sub>3</sub>, 20 HEPES, 25 glucose, 5 Na-ascorbate, 2 thiourea, 3 Na-pyruvate, 12 N-acetyl-L-cysteine, 2 MgSO<sub>4</sub>, 2 CaCl<sub>2</sub>, pH was adjusted to 7.3–7.4 with KOH or HCl if necessary) bubbled with 95% O<sub>2</sub>/5% CO<sub>2</sub>.

### Single-cell molecular biology of RTN neurons

Individual GFP- and/or mCherry-labeled RTN neurons were harvested under direct vision from mouse brainstem slices in the recording chamber of a fluorescence microscope (Zeiss Axioimager FS, Carl Zeiss Microscopy, White Plains, NY) for expression analysis of multiple genes by either multiplex nested single cell RT-PCR (sc-PCR) or multiplex quantitative sc-PCR (sc-qPCR), as described previously<sup>12,32</sup>. Intron-spanning, nested primer sets across splice sites for each gene of interest that were used in scPCR reactions were independently validated (Supplementary Table 1, for primer information), and no-template negative controls were included for each reaction. For sc-qPCR, primers that yielded short amplicons were utilized (Supplementary Table 2), cycle threshold (Ct) levels of test genes were re-scaled by their average, transformed into relative quantities using the amplification efficiency, normalized to *GAPDH* (an internal reference gene;  $Ct = Ct(\text{test}) - Ct(\text{GAPDH})$ ), and expressed as  $2^{-Ct}$ <sup>33</sup>.

### Virus production

We used lentivirus to infect neurons of the RTN and preBötC for shRNA-mediated knockdown (of PACAP, *Adcyap1*; and PAC1, *Adcyap1r1*) and for PACAP re-expression and

Cre expression in the RTN. For cell-specific transduction of Phox2b-expressing RTN neurons, we prepared a customized lentivirus targeting vector that included an artificial promoter, PRSx8, which incorporates 8 repeats of a Phox2a/b binding element<sup>12,13</sup>. For knockdown experiments, the PRSx8 promoter was used to drive expression of a PACAP shRNA hairpin sequence (see Supplementary Table 3) that was embedded in a mir30a site within an artificial intron, along with mCherry<sup>12</sup>. For PACAP re-expression in RTN neurons, the targeting construct was modified to replace the artificial intron with the PACAP coding sequence, an IRES and mCherry (*Mm Adcyap1* cDNA from MGC, Clone ID: 6829765; Dharmacon, MMM1013–202799047). For Cre expression in RTN neurons, we used a previously described PRSx8-Cre virus, modified to include an IRES-mCherry reporter<sup>4</sup>. For knockdown of PAC1 in preBötC neurons, we incorporated a PAC1 shRNA downstream of an EF1 $\alpha$  promoter in pLVTHM (gift from Didier Trono; Addgene plasmid # 12247)<sup>14,34</sup>. To test each shRNA hairpin, HEK293T cells were co-transfected with the viral targeting construct and an expression construct with the cognate cDNA (PACAP, as above; *Mm* PAC1 cDNA from MGC, Clone ID: 6852762; Dharmacon, MMM1013–202859842); we used qRT-PCR to determine knockdown efficiency at 72 h of 90% and 70% for PACAP and PAC1, respectively.

Replication-deficient high-titer lentivirus was produced in-house. Briefly, HEK293T cells were transfected with a pseudotyping envelope plasmid and a second generation packaging plasmid (pMD2.G, psPAX2; gifts from Didier Trono; Addgene 12259, 12260). The viral supernatant was harvested 48–72 h later, when transfection efficiency was ~100% (gauged by mCherry fluorescence). The virus was purified by low speed centrifugation and syringe filtration (Millipore Sigma SLHV033RS) to remove cellular debris, and then concentrated by ultra-centrifugation (30,000 RPM, 2.5h, 4°C; Beckman SW 41 Ti rotor). The pellet was re-suspended in DMEM and the virus was stored at –80°C. For titer estimation, we incubated HEK293T cells with a dilution series of virus and counted the number of fluorescent cells ( $\sim 5.0 \times 10^{10}$  TU/ml).

### Lentivirus injection into the mouse RTN and preBötC

Adult Phox2b::GFP and Phox2b::Cre;PACAP<sup>fl/fl</sup> mice (8–11 weeks old) were anesthetized with ketamine/dexmedetomidine HCl (100 mg/kg and 0.2 mg/kg, i.p.), mounted in a stereotaxic apparatus and maintained at 37°C with a servo-controlled heating pad. After craniotomy, a pipette filled with lentivirus (diluted to  $\sim 2 \times 10^9$  TU/ml) was inserted at coordinates  $\sim 1.4$  mm lateral to midline, 1.0 mm caudal to lambda and 5.2–5.5 mm ventral to the pial surface of the cerebellum<sup>29</sup>. In addition to stereotaxic coordinates, we recorded antidromic field potentials elicited by stimulating the mandibular branch of the facial nerve to locate the position of the facial motor nucleus more precisely. For bilateral injections in the RTN, the tip of the injection pipette was positioned 100  $\mu$ m below the facial motor nucleus<sup>12,14</sup>, and at each of 3 rostro-caudally aligned sites separated by 200  $\mu$ m. For preBötC injections, the pipette was positioned 700  $\mu$ m behind the caudal end of the facial motor nucleus and 4.95 to 5.25 mm ventral to the pial surface of the cerebellum, with bilateral injections at two rostrocaudal sites, separated by 100  $\mu$ m. In a subset of mice used for subsequent PACAP injection and dEMG recording, control and PAC1 shRNA virus was injected unilaterally. The glass injection pipette was connected to an electronically-

controlled pressure valve (Picospritzer II) and brief pressure pulses (3–6 ms) were used to inject 100–150 nl of virus. After surgery, mice were treated with ampicillin (100 mg/kg, sc), atipamezole (2 mg/kg, sc), and ketoprofen (4 mg/kg, sc). At least 4 weeks elapsed following virus injection before mice were examined in ventilatory and histochemical assays.

### Breathing measurements

Ventilatory responses were measured in conscious, unrestrained adult and neonatal mice by whole body plethysmography (EMKA Technologies, Falls Church, VA)<sup>12</sup>. A mass flow regulator (Alicat Scientific, Tucson, AZ) provided quiet, constant and smooth flow through the animal chamber (adult: 0.5 l/min; neonate: 0.1 l/min.). Mice were habituated to the plethysmography chamber for 4 h the day prior to testing and again for 2–3 h immediately before the test protocol. For adult mice, the protocol entailed an initial period in hyperoxia (1 h, 100% FiO<sub>2</sub>) followed by three sequential incrementing CO<sub>2</sub> challenges (7 min exposures to 4%, 6%, 8% CO<sub>2</sub>, balance O<sub>2</sub>; each separated by 5 min of 100% O<sub>2</sub>). For hypoxia challenges, mice were exposed to 10% O<sub>2</sub>, balance N<sub>2</sub> for up to 15 min. For neonatal mice, specialized chambers were used that were smaller in volume than the adult mouse chambers (Data Sciences International, St. Paul, MN) and outfitted with a custom remote video monitoring/recording system time-linked to the plethysmography data acquisition. The neonatal chambers contained a built-in warming pad that, together with placement of incandescent heating lamps, maintained the chamber at elevated baseline ambient temperature (26°C). An initial acclimation period for neonatal mice in hyperoxia (30–60 min in 60% O<sub>2</sub>, balance N<sub>2</sub>) preceded 6 min challenges in hyperoxic hypercapnia (10% CO<sub>2</sub>, 60% O<sub>2</sub>, balance N<sub>2</sub>), in hypoxia (12% O<sub>2</sub>, balance N<sub>2</sub>) and in normoxia (21% O<sub>2</sub>, balance N<sub>2</sub>), each separated by 6 min of hyperoxia (60% O<sub>2</sub>, balance N<sub>2</sub>). To test effects of temperature variations (from 22°C to 38°C) on apnea incidence, heating lamps were moved closer or further from the chambers; the chamber temperature was monitored using a thermometer (Thermalert TH-5), a temperature logger (DS1923-F5#, Thermochron, Baulkham Hills, AU) and followed in real time with the plethysmography software (iOX/EMKA, EMKA Technologies). Absolute measures of V<sub>T</sub> by plethysmography can be imprecise, especially in neonates, but the range of V<sub>T</sub> values we obtained aligns well with published values<sup>35,36</sup>; in addition, relative comparisons were made across experimental groups, and in individual mice under control conditions and CO<sub>2</sub> exposure. For both adults and neonates, hypercapnic exposure was performed in hyperoxia to minimize contributions of peripheral chemoreceptors to the hypercapnic ventilatory reflex<sup>37,38</sup> and attribute ventilatory effects primarily to central chemoreceptors.

### Analysis of responses to ventilatory challenge

Ventilatory flow signals were recorded, amplified, digitized and analyzed using iOX 2.10 (EMKA Technologies) to determine ventilatory parameters over sequential 20 s epochs (~50 breaths), during periods of behavioral quiescence and regular breathing. Minute ventilation (V<sub>E</sub>, ml/min/g) was calculated as the product of respiratory frequency (fR, breaths/min) and tidal volume (V<sub>T</sub>, ml/breath), and normalized to body weight (g). For analysis of the basal V<sub>E</sub> in hyperoxia, or acute hypercapnic ventilatory response, we sampled 10 consecutive epochs (200 s, representing ~400–500 breaths at rest) that showed the least inter-breath irregularity during the steady-state plateau period after each CO<sub>2</sub> exposure, as determined by

Poincaré analysis. For neonates, we obtained measurements from periods of time when the mice were visibly quiescent. The response to hypoxia was determined from the peak  $V_E$  during the hypoxic exposure (from a 20 s epoch at ~30 s to 1 min)<sup>12</sup>. Analysis was performed by individuals blinded to treatment and/or genotype.

### Apnea analysis

The frequency of apneic episodes was determined in periods (30–60 min) of quiescent breathing under hyperoxic conditions (adults: 100% O<sub>2</sub>, neonates: 60% O<sub>2</sub>) or in neonates under normoxic conditions (21% O<sub>2</sub>) while varying ambient temperature (22°C–38°C). Raw respiratory waveform data was processed off-line using Spike2 software (Cambridge Electronic Design, UK). Apneas identified by the software were manually verified. Spontaneous apneas were operationally defined as periods with an expiratory time >0.8 s that were not preceded by a sigh; this equates to the time for ~2 normal breath cycles, since the breathing frequency for BL6/J mice during quiet breathing is 160 breaths/min, or ~370 ms/breath. Individuals quantifying apneas were blinded to treatment and/or genotype; data from individual mice at different ages (P2–P5, P6–P9, P10–P12) were averaged, and treated as a single data point for analysis.

### In vivo hypercapnia-induced Fos expression

*In vivo* activation by CO<sub>2</sub> of RTN and preBötC neurons was assessed in adult Phox2b::GFP mice (P60–P100) by Fos protein or mRNA expression<sup>12</sup>. Mice were habituated to the plethysmography chamber for 4 h one day before and again 2 h prior to CO<sub>2</sub> exposure. When used for Fos immunohistochemistry, mice were exposed for 45 min to hypercapnia (12% CO<sub>2</sub>, 60% O<sub>2</sub>, balance N<sub>2</sub>) followed by 45 min of hyperoxia (60% O<sub>2</sub>, balance N<sub>2</sub>). When used for ISHH, mice were exposed to hypercapnia for 35 min without a subsequent hyperoxic exposure period. Mice were anesthetized with ketamine and xylazine (200 mg/kg and 14 mg/kg, i.p.), perfused transcardially with 4% paraformaldehyde/0.1 M phosphate buffer and their brainstems were cut on a vibrating microtome (VT1000S; Leica Biosystems, Buffalo Grove, IL) into 30 µm coronal or parasagittal sections. For immunostaining, we first detected GFP, mCherry, or SST by indirect immunofluorescence (primary and secondary antibodies listed in Supplementary Table 4). Subsequently, sections were incubated overnight with Fos primary antibody (goat anti-Fos, Santa Cruz sc-52-G), 1 h with biotinylated secondary antibody (donkey anti-goat, 705–065-147; Jackson ImmunoResearch, West Grove, PA) and 45 min with avidin-HRP (PK6100, Vector Labs, Burlingame, CA) followed by development of nickel-intensified 3, 3'-diaminobenzidine reaction product. For detection of *Fos* transcripts by fluorescence *in situ* hybridization, sections were mounted on charged slides, dried overnight and reacted following protocols described in Multiplex *in situ* hybridization histochemistry).

### In vivo PACAP injections in the preBötC

To determine respiratory effects of PACAP injections into the preBötC of adult mice, we used a similar approach as described above for viral injections, but with additional diaphragm electromyography (dEMG) measurements as an indication of central respiratory output as previously described<sup>39</sup>. Thus, anesthetized mice (ketamine/dexmedetomidine HCl; 100 mg/kg, 0.2 mg/kg, i.p.) were mounted in a stereotaxic apparatus, maintained at

37°C with a servo-controlled heating pad, and wire hook electrodes were placed bilaterally in the diaphragm. A combination of stereotaxic coordinates and antidromic facial field recordings was used to identify the preBötC region (see above) for placement of a pressure-injection pipette containing vehicle (PBS) or PACAP-38 (10 µM in PBS; 4031157, Bachem, Torrance, CA) and rhodamine-labeled latex beads (Lumafluor, Durham, NC); brief pressure pulses (3–6 ms; Picospritzer II) were used to inject PBS (30 nl), DL-homocysteic acid (10 nl, 4 mM, 40 pmol) or PACAP (10 µM, 0.3 pmol). Analog recordings of dEMG activity (bandpass, 300–3000 Hz) were acquired on a computer via a Micro1401 digitizer (Cambridge Electronic Design) and processed off-line using Spike2 software (v. 8.0; Cambridge Electronic Design) to digitally filter the EKG artifact, and to rectify and integrate the dEMG signal (time constant, 0.03 s). The respiratory frequency (fR) was triggered from the integrated EMG signal and dEMG burst amplitude was measured using a peak detection feature of the Spike 2 software, with fR and dEMG amplitude taken as an index of overall inspiratory neural output (in arbitrary units). After dEMG recording, mice were immediately perfused, and brainstem sections processed for SST and choline acetyltransferase (ChAT) immunohistochemistry to determine the location of the injection relative to the preBötC.

### In vitro PACAP injections in the preBötC

Rhythmically-active medullary slices were prepared from neonatal FVB mice (postnatal day 0–3 and P9–10) using methods similar to those described previously<sup>40–42</sup>. Briefly, animals were anesthetized with isoflurane and the brainstem-spinal cord was isolated in cold (4°C) artificial cerebrospinal fluid (aCSF) containing (in mM): 120 NaCl, 3 KCl, 1.25 NaH<sub>2</sub>PO<sub>4</sub>, 1 CaCl<sub>2</sub>, 2 MgSO<sub>4</sub>, 26 NaHCO<sub>3</sub>, 20 D-Glucose and bubbled with 95% O<sub>2</sub>–5% CO<sub>2</sub>. The brainstem-spinal cord was placed on the chuck of a vibrating microtome (VT1200S; Buffalo Grove, IL) and serial, 100–200 µm sections were cut in the rostral to caudal direction. Sections were trans-illuminated to identify specific subnuclei of the inferior olive in the slice, which serve as markers of the rostral boundary of the preBötC<sup>42</sup> and a single 550 µm (P0–3) or 600 µm (P9–10) rhythmic transverse slice containing the preBötC was obtained. Slices were pinned, rostral surface up, in a 5 ml recording chamber, continuously perfused (100 ml recirculating, 8 ml min<sup>-1</sup>, 25 ± 1°C) and [K<sup>+</sup>] in the aCSF was increased to 5 mM or 9 mM<sup>42</sup>. Inspiratory-related motor activity was recorded via suction electrodes placed on the hypoglossal (XII) nerve rootlets and/or the rostral surface of the slice overlying the preBötC. Signals were amplified, band-pass filtered (300 Hz to 1 kHz), rectified, and integrated. Data were acquired using Axoscope 9.2 and a Digidata 1322 A/D (Molecular Devices, Sunnyvale CA, USA).

Substance P (Tocris, Minneapolis, MN) and PACAP (Bachem) were prepared in aCSF ([K<sup>+</sup>] = 5 or 9 mM to match the aCSF) as stock solutions and frozen until needed. Drugs were applied unilaterally via pressure injection from triple-barreled pipettes (5–6 µm outer diameter per barrel, borosilicate glass capillaries, World Precision Instruments, Sarasota, FL, USA). Microinjections were controlled by a programmable stimulator (Master-8; A.M.P.I., Jerusalem, Israel) connected to a Picospritzer (Spritzer4 Pressure Micro-Injector). Consecutive drug applications were separated by a minimum of 15 min. Substance P (1 µM, 10 s, ~30 nl) was locally applied to identify the preBötC based on a characteristic immediate, increase in inspiratory frequency (>2-fold)<sup>43</sup> as the injection site was moved in

a grid-like fashion until the characteristic response was observed. PACAP-38 (0.1, 1.0 and 10  $\mu\text{M}$  in aCSF with 5 or 9 mM  $\text{K}^+$ ; Bachem 4031157) was injected at the identified site (30 sec,  $\sim 90$  nl; 60 sec,  $\sim 180$  nl). Drug effects on preBötC frequency were assessed off-line using pCLAMP 9.2 (Clampfit, Molecular Devices) and Microsoft Excel. Frequency values are reported relative to baseline (average instantaneous frequency over the minute immediately preceding the drug-injection); response time course was obtained by averaging instantaneous frequency into 30 s bins, and peak relative frequency by a moving average of 6 consecutive bursts.

### In vitro recordings of pH sensitivity of RTN neurons

Cell-attached recordings of pH sensitivity of GFP-labeled RTN neurons were performed in transverse brain slices (300  $\mu\text{m}$ ) prepared from neonatal Phox2b::Cre;Phox2b::GFP;PACAP<sup>fl/fl</sup> mice (P4-P16), as previously described<sup>12,14</sup>. Slices were placed in a chamber on a fixed-stage fluorescence microscope equipped with fluorescence and infrared Nomarski optics (Zeiss Axio Examiner) at room temperature in HEPES-based buffer (mM): 140 NaCl, 3 KCl, 2  $\text{MgCl}_2$ , 2  $\text{CaCl}_2$ , 10 HEPES, 10 glucose, with pH adjusted between 7.0 and 8.0 by addition of HCl or NaOH. Patch electrodes (3–6 M $\Omega$ ) for cell-attached recordings were filled with (mM): 120  $\text{KCH}_3\text{SO}_3$ , 4 NaCl, 1  $\text{MgCl}_2$ , 0.5  $\text{CaCl}_2$ , 10 HEPES, 10 EGTA, 3 Mg-ATP, and 0.3 GTP-Tris (pH 7.2, adjusted with KOH). Firing activity was recorded using pCLAMP software, a Multiclamp 700A amplifier and Digidata 1440A digitizer (Molecular Devices). All recordings were made in the presence of strychnine (30  $\mu\text{M}$ ), bicuculline (10  $\mu\text{M}$ ), and 6-cyano-7-nitroquinoxaline-2,3-dione (CNQX, 10  $\mu\text{M}$ ). Firing rate histograms of RTN neuronal discharge were generated by integrating action potential discharge in 10 s bins using Spike2 software (Cambridge Electronic Design), and the pH sensitivity of individual RTN neurons was assessed by linear regression analysis to obtain a pH<sub>50</sub> value (i.e., pH at which firing rate was half that obtained at pH 7.0)<sup>12,14</sup>. A subset of recorded cells was harvested following recording for multiplex sc-qPCR, as described<sup>12</sup>. The recordings and analysis were performed by investigators blinded to the Cre genotype of Phox2b::Cre;Phox2b::GFP;PACAP<sup>fl/fl</sup> littermates.

### Multiplex in situ hybridization histochemistry (ISHH)

Multiplex fluorescent *in situ* hybridization was performed as described previously<sup>6</sup>. Mice were anesthetized (ketamine/dexmedetomidine HCl; 100 mg/kg, 0.2 mg/kg, i.p.), perfused transcardially with 4% paraformaldehyde and post-fixed in the same fixative overnight at 4°C. Brainstem sections were cut (30  $\mu\text{m}$ ), mounted onto charged slides and dried overnight, before processing according to manufacturer instructions for RNAscope® (Advanced Cell Diagnostics Newark, CA, SCR\_012481). In most cases, sections were incubated for 2 h at 40°C with catalog oligonucleotide probes targeting transcripts (Supplementary Table 5): PACAP (*Adcyap1*); PAC1 (*Adcyap1r1*); VGlut2 (*Slc17a6*); *Sst*; *Phox2b*; *Fos*; *Glutamate decarboxylases 1 and 2* (*Gad1*, *Gad2*); *Aldehyde dehydrogenase family 1, member L1* (*Aldh1l1*); and *microtubule-associated protein 2* (*Map2*). After incubation with probes, tissue was treated according to the manufacturer's protocol (ACD). The presence of residual, recombined PACAP transcript in Cre-positive Phox2b::Cre;PACAP<sup>fl/fl</sup> mice (see Extended Data Fig 1b) was detected by the catalog RNAscope probe for *Adcyap1*. Therefore, to demonstrate effective Cre recombination by ISHH we obtained a custom-designed probe

targeting the short, deleted exon 2 region of the recombined transcript, and modified the RNAscope protocol by reducing the probe incubation time to 1h.

When combined with detection of GFP, mCherry, ChAT or SST, sections were first subjected to the ISHH protocol and then rinsed  $2 \times 2$  min in blocking buffer (10% horse serum, 0.1% triton in 100 mM Tris buffer), incubated for 1 h in blocking buffer containing primary antibodies. Sections were rinsed  $2 \times 2$  min in Tris buffer, incubated for 30 min in Tris buffer with secondary antibodies, rinsed and allowed to air dry. Slides were covered with Prolong Gold with DAPI Anti-fade mounting medium (Molecular Probes, Eugene, OR).

### Cell counts and analysis

Serial coronal sections (1:3 series) through the rostrocaudal extent of the RTN were mounted on glass slides, and images were acquired using an epifluorescence microscope (Zeiss Axioimager Z1, Carl Zeiss Microscopy) equipped with Neurolucida software (MBF Bioscience, Williston, VT); images were assembled for presentation using Photoshop (v. 19–21) and CorelDraw (v. 17). Labeled neurons were counted and aligned for averaging according to defined anatomical landmarks<sup>29</sup>. No stereological correction factor was applied. Averaged cell counts obtained from multiple sections from each mouse were treated as a single data point for subsequent analysis. For virus injections in the preBötC (see Extended Data Figs. 5c,d, 6a,b), we outlined the region in parasagittal brainstem sections that contained mCherry-labeled neurons, traced those onto the relevant sections of the mouse atlas (Figs 111 and 112 of<sup>29</sup>) using Photoshop and ImageJ to estimate the fractional coverage of the preBötC region (according to anatomical landmarks and SST immunohistochemistry, mapped onto the same sections). The investigator assessing and quantifying cellular profiles and transduced regions was blinded to treatment and/or genotype.

### Timed pregnancy and induction of pre-term birth in mice

In order to obtain mouse pups at precise embryonic stages, we paired male and female Phox2b::GFP mice overnight and verified the start of gestation by the appearance of a copulation plug. For inducing pre-term birth, we used the antiprogestin RU486 (mifepristone), following procedures outlined in<sup>19</sup>. Thus, from a stock of RU486 (10 mM in absolute ethanol), we prepared a 150 µg/ml solution in sterile water and made a single injection (1 ml, sc) of that diluted sterile solution into the interior left or right flank of the pregnant dam (e16.5-e18.5). Pups were typically delivered within 24 h of the RU486 injection (1–3 days pre-term), at which point they were either transcidentally perfused for multiplex ISHH or rapidly decapitated to prepare brainstem slices for neuron harvesting and multiplex single cell qRT-PCR.

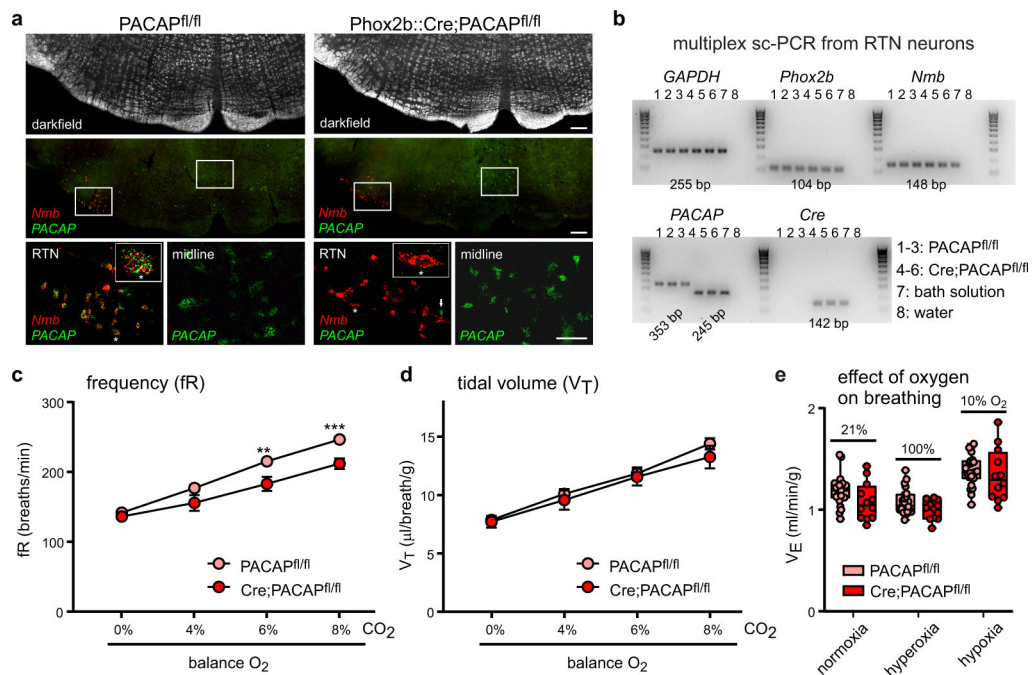
Animals obtained while still within the amniotic sac were transferred immediately following birth to ice-cold HEPES-buffered saline, and the amniotic membranes were manually removed. For ISHH, animals were transcidentally perfused by gravity flow with 1 ml heparinized phosphate-buffered saline followed by 1–2 ml 4% paraformaldehyde; the brains were removed from the skull using a dissection microscope, post fixed overnight in 4%

paraformaldehyde at 4°C, sectioned on a vibratome and then processed for ISHH. For quantitative single cell PCR, the head was removed, transferred to oxygen-bubbled dissection solution and, after recovering 1–2 other pups in similar fashion, the brains were extracted and prepared for slice preparation. For litters in which the dam extracted the pups from the amniotic sac, pups were transferred to heated bedding for pre-determined periods of time, anesthetized by hypothermia on ice for five minutes, and then either transcardially perfused and processed for ISHH or decapitated for brain slice preparation and single cell harvest, as described above.

## Statistics

Results are presented as mean  $\pm$  SEM, or in box and whiskers plots (i.e., median bisecting a box bounded by 25<sup>th</sup> and 75<sup>th</sup> percentile, with whiskers representing the range). All statistical analyses were performed using GraphPad Prism (v. 8.2, GraphPad Software, San Diego, CA), with parametric tests employed for normally-distributed datasets. Details of specific tests are provided in the text or figure legends. Statistical significance was set at  $P < 0.05$ .

## Extended Data



### Extended Data Figure 1. Validation of PACAP recombination in RTN neurons from Phox2b::Cre;PACAP<sup>fl/fl</sup> mice.

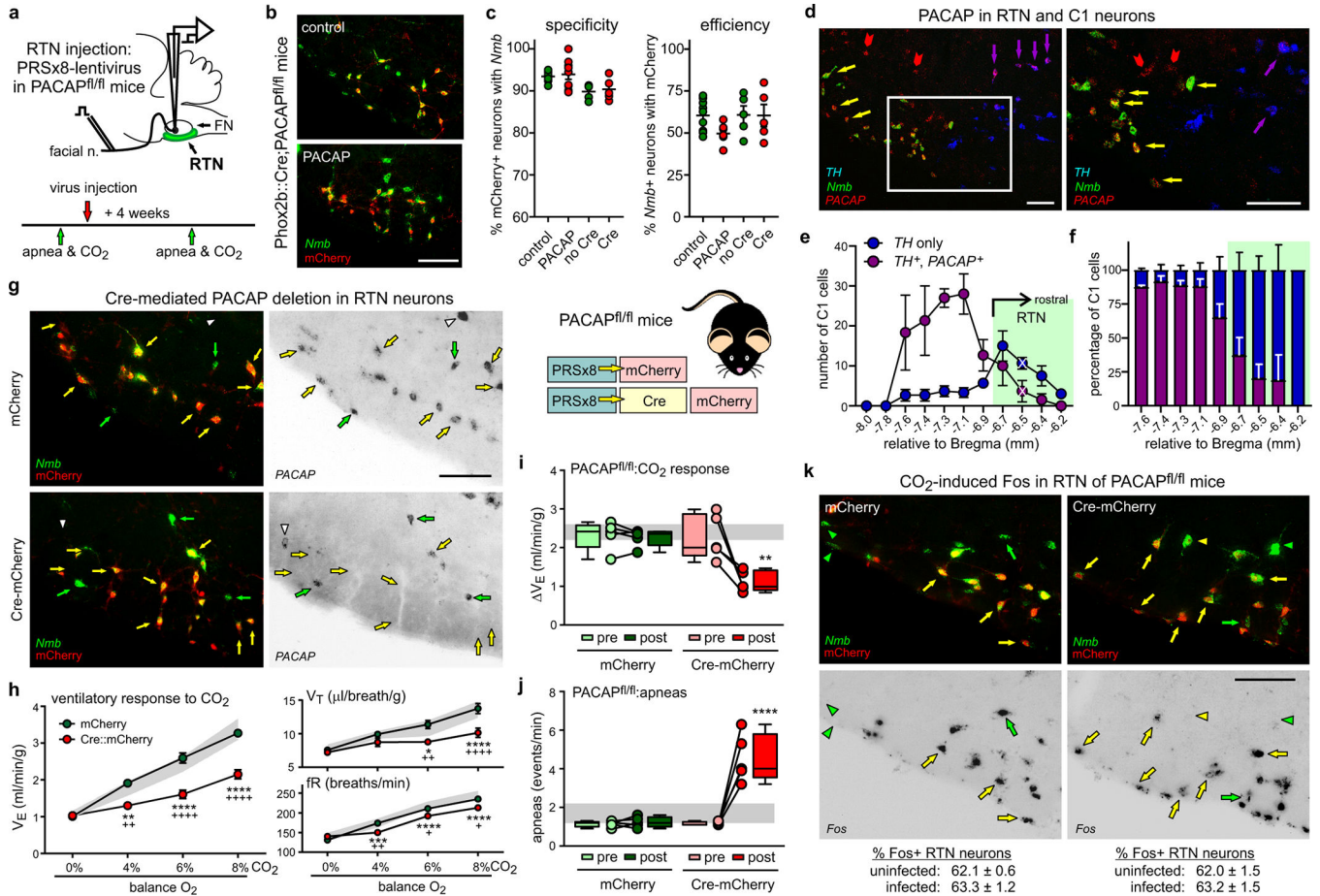
**a.** Multiplex *in situ* hybridization for *PACAP* and *Nmb* in the ventral brainstem of Phox2b::Cre;PACAP<sup>fl/fl</sup> mice that were either Cre-negative (*left*) or Cre-positive (*right*). The boxed areas in low-power fluorescence images (*middle*) are expanded in higher power images (*lower*) to reveal selective *PACAP* deletion from *Nmb*-expressing RTN neurons in Cre-positive mice, with no effect on *PACAP* expression in midline regions. *Nmb*<sup>+</sup> neurons indicated with *asterisk* are expanded in insets; *arrow* indicates non-*Nmb*<sup>+</sup> cell that expresses

**PACAP.** Data representative of two replicate experiments from each of three Cre-negative and Cre-positive mice. Coronal section, scale bars = 200  $\mu$ m and 100  $\mu$ m.

**b.** Single cell RT-PCR of GFP-labeled RTN neurons, verified by expression of *Phox2b* and *Nmb*, from control Cre-negative PACAP<sup>fl/fl</sup> mice (lanes 1–3) and Phox2b::Cre;PACAP<sup>fl/fl</sup> mice (lanes 4–6). PACAP transcripts from Cre-positive RTN neurons were smaller, as expected for excision of exon 2; when recombined, this excision creates a frameshift mutation<sup>10</sup>. Data representative of 16 cells from Cre-negative and Cre-positive mice (N=2 each).

**c,d.** Effects of raised ambient CO<sub>2</sub> (FiCO<sub>2</sub>, 4%–8%; balance O<sub>2</sub>) on respiratory frequency (**c**: fR, breaths/min, mean  $\pm$  SEM) and tidal volume (**d**: V<sub>T</sub>,  $\mu$ l/breath/g, mean  $\pm$  SEM) in PACAP<sup>fl/fl</sup> (N=23) and Phox2b::Cre;PACAP<sup>fl/fl</sup> mice (N=12). V<sub>T</sub>: F<sub>1,33</sub>=0.5134, P=0.4787; fR: F<sub>1,33</sub>=10.22, P=0.0031, \*\*, P=0.0013, \*\*\*, P=0.0005 for PACAP<sup>fl/fl</sup> vs. Cre;PACAP<sup>fl/fl</sup> by 2-way RM ANOVA (Sidak multiple comparison).

**e.** Ventilation (V<sub>E</sub>, ml/min/g; median, 25–75%ile with minima and maxima) in varied ambient O<sub>2</sub> (normoxia: FiO<sub>2</sub>, 21%; hypoxia: FiO<sub>2</sub>, 10%; hyperoxia: FiO<sub>2</sub>, 100%) for PACAP<sup>fl/fl</sup> (N=23) and Phox2b::Cre;PACAP<sup>fl/fl</sup> mice (N=12). F<sub>1,99</sub>=5.332, P=0.0230, for PACAP<sup>fl/fl</sup> vs. Cre;PACAP<sup>fl/fl</sup> by 2-way ANOVA (NS, Sidak multiple comparison).



**Extended Data Figure 2. Effects of Cre-mediated deletion of PACAP in RTN neurons of adult mice on breathing and CO<sub>2</sub>-evoked neuronal activation in vivo.**

- a.** Schematic depicting approach for PRSx8 promoter-driven lentiviral injections in PACAP<sup>fl/fl</sup> mice using stereotaxic coordinates and antidromic facial field potentials to locate the RTN. Outline of experimental design for recording physiological responses before and 4 weeks after lentivirus injections.
- b.** Virally-infected (mCherry<sup>+</sup>) RTN neurons (*Nmb*<sup>+</sup>) in Phox2b::Cre;PACAP<sup>fl/fl</sup> mice injected with control or PACAP-expressing lentivirus. Coronal section, scale bar=100 μm (N=9 mice each).
- c.** Quantification of viral transduction specificity (% of mCherry-labeled neurons in the RTN region that were *Nmb*<sup>+</sup>) and efficiency (% of *Nmb*-expressing neurons that were mCherry<sup>+</sup>) in mice injected with lentivirus expressing mCherry (control) or PACAP (N=9 each), or mCherry (no Cre) and Cre-mCherry (N=5 each).
- d.** Multiplex *in situ* hybridization for *PACAP*, *Nmb* and *TH* in the caudal RTN region of the rostral ventrolateral medulla (-6.5 mm, relative to Bregma); boxed area from low-power merged image is expanded (*right*) to show that *Nmb*-expressing RTN neurons universally express *PACAP* (*yellow arrows*) whereas only few *TH*-expressing C1 neurons express *PACAP* in this region and most *PACAP*-expressing C1 cells are located mediodorsal to the RTN (*purple arrows*). *PACAP* is also expressed in non-RTN, non-C1 cells (*red arrowheads*). Representative of 3 independent experiments (as quantified in **e,f**). Coronal section, scale bars = 100 μm
- e,f.** Cell counts from *in situ* hybridization experiments (N=3) through the C1 region quantifying *TH*-expressing C1 neurons that also express *PACAP* (**e**; mean ± SEM), and the percentage of *PACAP*-expressing C1 neurons (**f**; mean ± SEM). Note that most neurons in the caudal C1 express *PACAP*, whereas progressively fewer rostral C1 neurons express *PACAP* in the region that overlaps with the RTN. (X marks the approximate rostrocaudal level depicted in **d**).
- g.** Multiplex *in situ* hybridization for *PACAP* and *Nmb* combined with immunostaining for mCherry in the RTN region of PACAP<sup>fl/fl</sup> mice that were injected with virus for mCherry or Cre-mCherry (schematic on right). Transduced RTN neurons are indicated by *yellow arrows* and uninfected RTN neurons by *green arrows*. Coronal section, scale bar = 100 μm.
- h.** Effects of raised ambient CO<sub>2</sub> (FiCO<sub>2</sub>, 4%–8%; balance O<sub>2</sub>) on ventilation (V<sub>E</sub>, ml/min/g; mean ± SEM), respiratory frequency (fR, breaths/min; mean ± SEM) and tidal volume (V<sub>T</sub>, μl/breath/g; mean ± SEM) in PACAP<sup>fl/fl</sup> injected in the RTN with control (mCherry) or Cre-mCherry lentivirus. Phox2b::Cre;PACAP<sup>fl/fl</sup> mice (N=5 each). The 95% CI are from all mice prior to virus injection. V<sub>E</sub>: F<sub>2,68</sub>=47.38, V<sub>T</sub>: F<sub>2,68</sub>=16.22, fR: F<sub>2,68</sub>=23.05, all P<0.0001 for treatment main effects; \*, P<0.05, \*\*, P<0.005, \*\*\*, P<0.001, \*\*\*\*, P<0.0001 for Cre vs. initial; +, P<0.05, ++, P<0.005, +++, P<0.0001 for Cre vs. no Cre, by 2-way ANOVA (Tukey's multiple comparison).
- i,j.** CO<sub>2</sub>-evoked change in V<sub>E</sub> (**i**) and apnea frequency (**j**) in PACAP<sup>fl/fl</sup> mice prior to and 4 weeks following RTN injection of control (mCherry) or Cre-mCherry lentivirus (N=5 each; as in Fig. 1d). V<sub>E</sub>: F<sub>3,16</sub>=11.39, P=0.0003; apnea: F<sub>3,16</sub>=34.3, P<0.0001 by ANOVA; \*\*, P=0.012 (**i**) and \*\*\*\*, P<0.0001 (**j**) Cre-mCherry vs. control or pre-injection (Tukey's multiple comparison). Box-and-whisker plots in this and other panels define the median, the 25–75%ile, and the minima and maxima. The shaded regions depict 95% CI for uninjected PACAP<sup>fl/fl</sup> mice.



subset of mice expressing control (n=6) or PACAP shRNA (n=10). Box-and-whisker plots in this and other panels define the median, the 25–75%ile, and the minima and maxima.

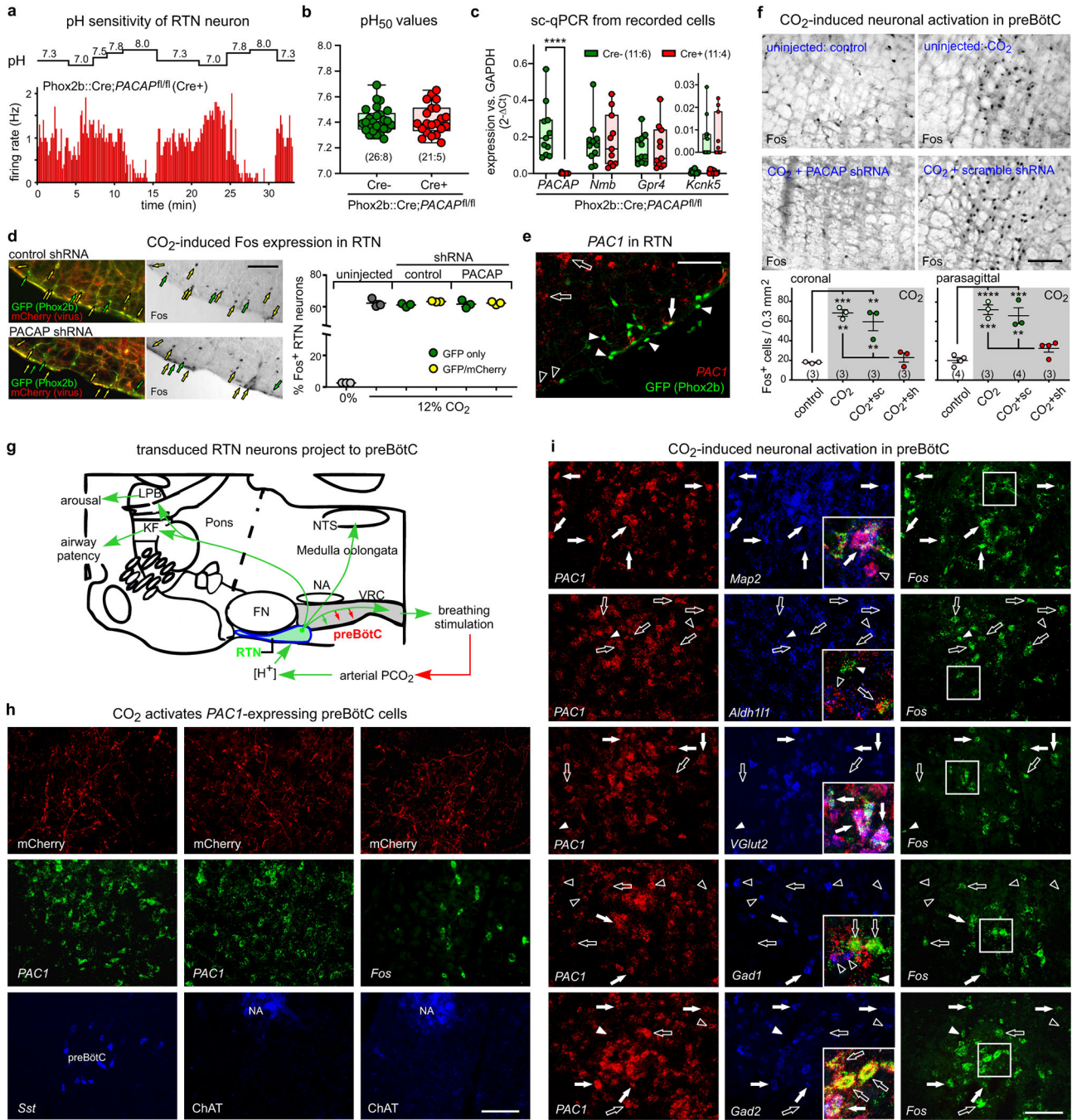
**c,d.** *In situ* hybridization combined with GFP and mCherry immunohistochemistry showing expression of transcripts for *PACAP* (**c**) or *VGlut2* (**d**) in RTN neurons transduced with lentivirus expressing control shRNA (*upper*) or PACAP shRNA (*lower*). Transduced RTN neurons indicated by *yellow arrows*, uninfected RTN neurons by *green arrows*. Data representative of two replicate experiments from mice injected with virus for control (N=6) and PACAP shRNA (N=10). Coronal section, scale bar = 100  $\mu$ m.

**e.** Schematic shows single GFP-expressing RTN neurons aspirated under direct vision into pipettes from brainstem slices, and processed for multiplex quantitative RT-PCR (*upper*). Cumulative frequency distribution of *PACAP* (*middle*) and *VGlut2* (*lower*) transcript levels from uninjected mice (GFP), or mice infected with either control or PACAP shRNA. Red arrow indicates % of cells infected with PACAP shRNA in which *PACAP* expression was undetectable. *Insets*: Individual cell expression levels for *PACAP* and *VGlut2* (relative to GAPDH; median and 95% CI, with number of cells: number of mice). \*\*\*\*,  $P < 0.0001$  vs. GFP & CON, by Kruskal–Wallis one-way ANOVA.

**f.** Effects of raised ambient  $\text{CO}_2$  ( $\text{FiCO}_2$ , 4%–8%; balance  $\text{O}_2$ ) on respiratory frequency (fR, breaths/min; mean  $\pm$  SEM) and tidal volume ( $V_T$ ,  $\mu\text{l}/\text{breath}/\text{g}$ ; mean  $\pm$  SEM) from mice prior to and 4 weeks following RTN injection with either control (n=9) or PACAP (n=13) shRNA-expressing lentivirus. fR:  $F_{3,160}=6.68$ ,  $P < 0.0001$ , for treatment by 2-way ANOVA; \*,  $P=0.0414$  in 4% and  $P=0.0272$  in 8%  $\text{CO}_2$ , \*\*,  $P=0.0011$ , for PACAP shRNA vs. initial (Tukey's multiple comparison).  $V_T$ :  $F_{3,160}=9.94$ ,  $P < 0.0001$ , for treatment by 2-way ANOVA. \*,  $P=0.0115$ , \*\*,  $P=0.0011$ , for PACAP shRNA vs. initial (Tukey's multiple comparison).

**g.**  $\text{CO}_2$ -evoked change in  $V_E$  in Phox2b::GFP mice prior to and 4 weeks following RTN injection of control (n=9) or PACAP shRNA (n=13) expressing lentivirus. \*\*\*\*,  $P=0.0002$  by two-sided Wilcoxon matched-pairs signed rank test.

**h.** Ventilation in varied ambient  $\text{O}_2$  (normoxia:  $\text{FiO}_2$ , 21%; hypoxia:  $\text{FiO}_2$ , 10%; hyperoxia:  $\text{FiO}_2$ , 100%) from mice 4 weeks following RTN injection with either control (n=9) or PACAP (n=13) shRNA-expressing lentivirus.  $F_{3,120}=0.1761$ ,  $P=0.9124$ , for treatment (control vs. PACAP shRNA) by 2-way ANOVA.



**Extended Data Figure 4. CO<sub>2</sub> sensitivity of RTN and preBötC neurons after PACAP depletion.**

**a.** Firing rate histogram from cell-attached recording of RTN neuron exposed to acidified and alkalinized bath solutions in brainstem slice from a Cre-positive Phox2b::Cre;PACAP<sup>fl/fl</sup> mouse.

**b.** The pH sensitivity of RTN neurons (pH<sub>50</sub>, pH where firing rate is half that obtained at pH 7.0) obtained from Phox2b::Cre;PACAP<sup>fl/fl</sup> mice that were Cre-negative or Cre-positive. (n cells: N mice; P=0.8248 by unpaired t-test). Box-and-whisker plots in this and other panels define the median, the 25–75% ile, and the minima and maxima.

**c.** Single cell qRT-PCR for the indicated transcripts from RTN neurons harvested after recordings of pH sensitivity in brainstem slices from Cre- or Cre+ Phox2b::Cre;PACAP<sup>fl/fl</sup> mice (n cells: N mice);  $F_{3,80}=7.729$ ,  $P=0.0001$  for interaction by 2-way ANOVA, \*\*\*\*  $P<0.0001$  for PACAP from Cre- vs. Cre+ mice.

**d.** *Left.* Mice injected with lentivirus for control (*upper*) or PACAP shRNA (*lower*) were exposed to CO<sub>2</sub> (12% CO<sub>2</sub>, 60% O<sub>2</sub>, balance N<sub>2</sub> for 45 min). Immunohistochemistry for GFP and mCherry (*left*), and Fos (*right*), reveals CO<sub>2</sub>-induced Fos expression in numerous uninfected (*green arrows*) and lentiviral-transduced RTN neurons (*yellow arrows*). *Right.* Percentage of Fos-immunopositive expressing RTN neurons (mean ± SEM) under control conditions (0% CO<sub>2</sub>) and after CO<sub>2</sub> exposure in uninjected mice (N=3 each), and in mice injected with lentivirus expressing either control or PACAP shRNA (N=3 each). Coronal section, scale bars = 100 μm.

**e.** GFP immunohistochemistry for Phox2b-expressing RTN neurons combined with *in situ* hybridization for *PAC1* receptor. *Filled arrow:* Phox2b-expressing RTN neuron associated with *PAC1*; *filled arrowheads*, Phox2b-expressing RTN neurons without *PAC1*; *empty arrow:* *PAC1*-expressing neuron outside the RTN. Data representative of experiments from 3 mice. Coronal section, scale bar = 100 μm.

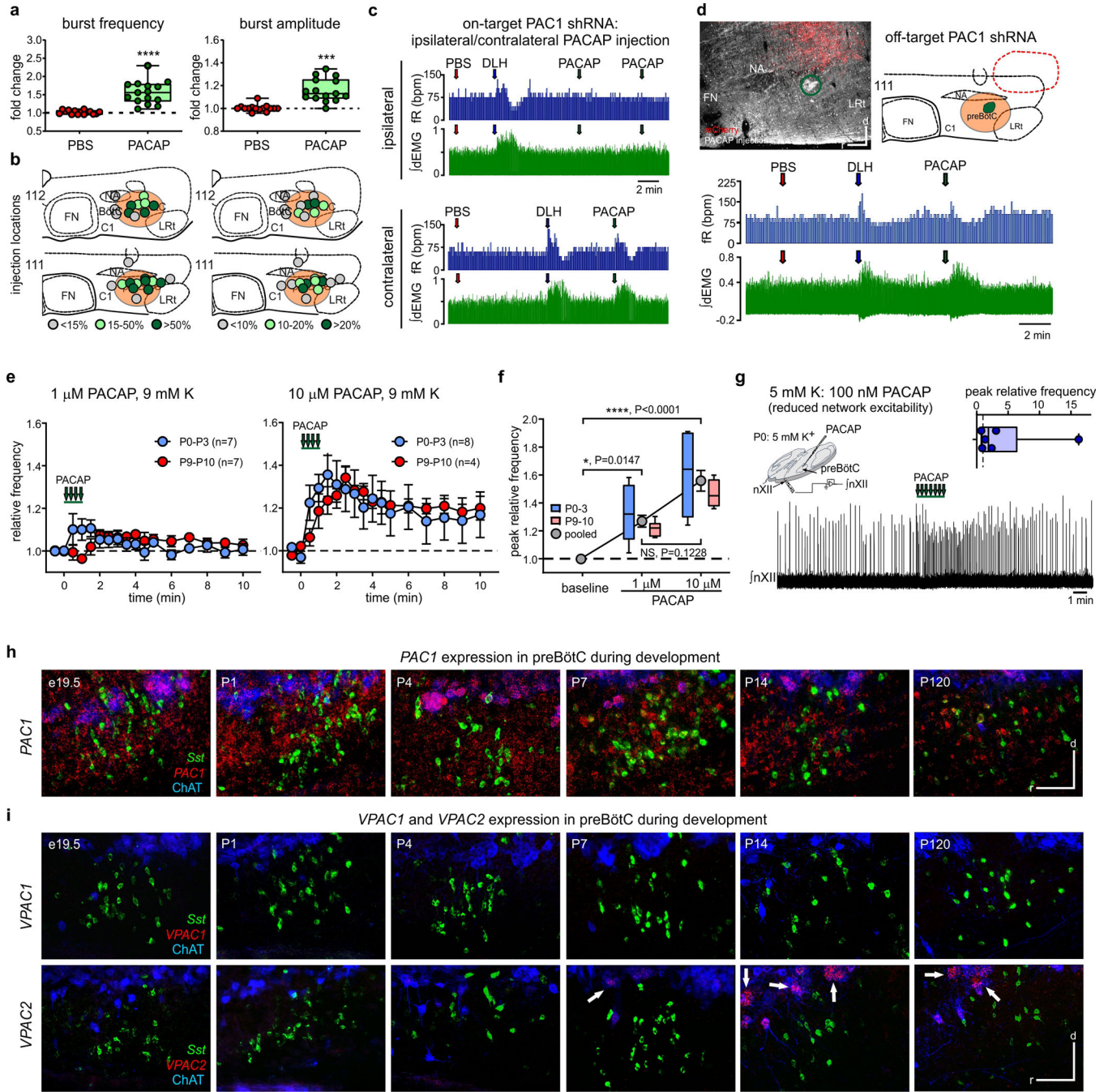
**f.** *Upper.* Fos immunolabeling in coronal brainstem sections from uninjected mice under control conditions and after CO<sub>2</sub> exposure, and in CO<sub>2</sub>-exposed mice that had received RTN injections of lentivirus expressing scrambled or PACAP shRNA. Scale bar = 100 μm. *Lower.* Quantification of Fos-immunolabeled cells in the preBötC region. Averaged cell counts (± SEM) were obtained from multiple sections in either coronal or parasagittal plane from individual mice and treated as a single data point for subsequent analysis (N=mice analyzed for each condition). Data from coronal and parasagittal sections were essentially identical and combined for subsequent analysis. For coronal:  $F_{3,8}=22.4$ ,  $P=0.003$  by ANOVA; control vs. CO<sub>2</sub>,  $P=0.0007$ ; control vs. CO<sub>2</sub>+sc,  $P=0.0027$ ; CO<sub>2</sub>+sh vs CO<sub>2</sub>,  $P=0.0015$ ; CO<sub>2</sub>+sh vs CO<sub>2</sub>+sc,  $P=0.0060$  (Tukey's multiple comparison). For parasagittal:  $F_{3,10}=27.25$ ,  $P<0.0001$  by ANOVA; control vs. CO<sub>2</sub>,  $P<0.0001$ ; control vs. CO<sub>2</sub>+sc,  $P=0.0003$ ; CO<sub>2</sub>+sh vs CO<sub>2</sub>,  $P=0.0009$ ; CO<sub>2</sub>+sh vs CO<sub>2</sub>+sc,  $P=0.0030$  (Tukey's multiple comparison).

**g.** Schematic in the parasagittal plane illustrating the location of CO<sub>2</sub>/H<sup>+</sup>-sensitive chemoreceptor neurons in the RTN and their projections to respiratory regions of the brainstem. NTS, nucleus tractus solitarius; LBP, lateral parabrachial nucleus; KF, Kölliker-Fuse.

**h.** Immunofluorescence labeling for mCherry and ChAT combined with multiplex *in situ* hybridization for *PAC1*, *Sst* and/or *Fos* in coronal sections containing the preBötC from mice injected in the RTN with lentivirus expressing control or PACAP shRNA. The preBötC was identified by its location relative to the nucleus ambiguus (i.e., see ChAT-IR) in a region with a high concentration of *Sst*-expressing neurons. The preBötC is innervated by fibers from lentivirus-infected RTN neurons (see mCherry staining), and contains cells that express *PAC1*. After exposure to elevated CO<sub>2</sub> (12%, 60% O<sub>2</sub>, balance N<sub>2</sub> for 35 min) preBötC cells express *Fos*. The data are representative of two replicate experiments from each of 6 mice tested for CO<sub>2</sub>-induced *Fos* expression after control lentivirus injection in RTN. Scale bar = 100 μm.

**i.** Histochemical localization of *PAC1* and CO<sub>2</sub>-induced *Fos* expression together with markers for neurons (*Map2*) or astrocytes (*Aldh1ll1*), and for excitatory (*VGlut2*) or

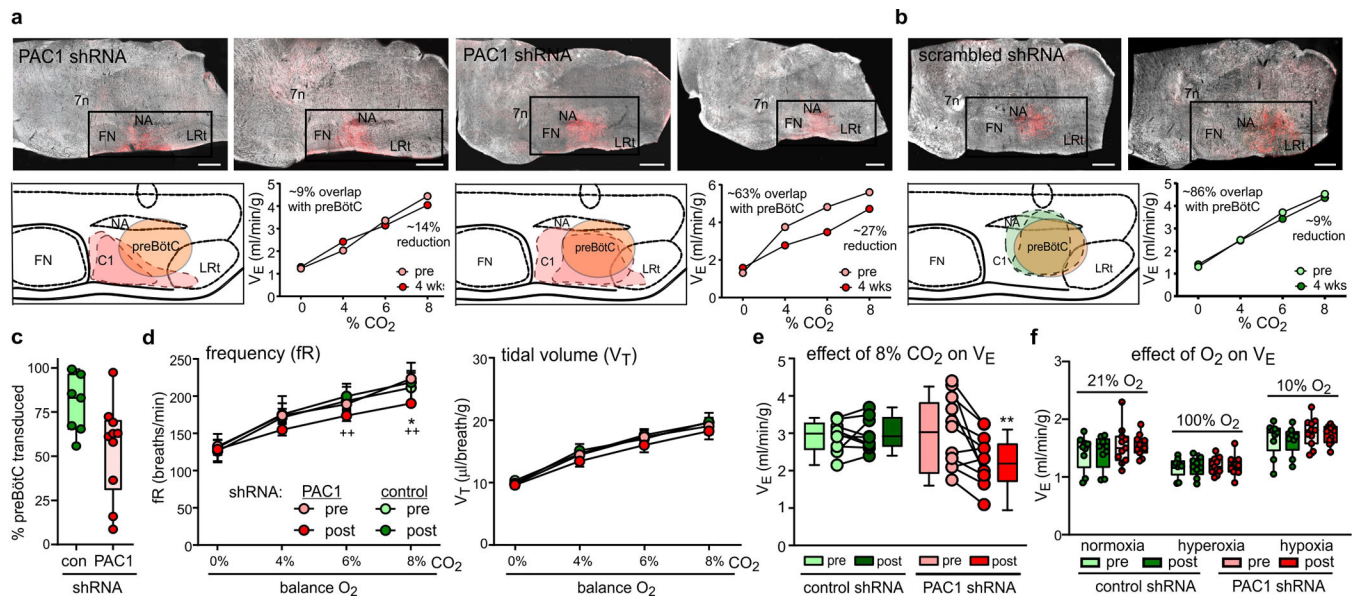
inhibitory neurons (*Gad1*, *Gad2*). *Insets*: merged images from boxed regions at higher magnification. *Filled arrows*: *PAC1*- and *Fos*-expressing cells containing the marker; *open arrows*: *PAC1*- and *Fos*-expressing cells without the marker; *filled arrowhead*: *Fos* with no *PAC1* or marker; *empty arrowhead*: *PAC1* cells containing the marker but no *Fos*. Data representative of two replicate experiments from each of 4 mice. Coronal section, scale bar = 100  $\mu\text{m}$ .



Extended Data Figure 5. Effect of PACAP injection in the preBötC on respiratory output.

- a.** Summary data illustrating effects of vehicle (PBS) and PACAP injections in the preBötC (n=15 injections, N=6 anesthetized mice) on dEMG burst frequency (fR) and burst amplitude. Data were normalized relative to control values before PBS. Box-and-whisker plots in this and other panels define the median, the 25–75%ile, and the minima and maxima. RM-ANOVA on absolute values for fR;  $F_{2,28}=62.71$ , \*\*\*\*,  $P<0.0001$  for PACAP vs. control and PBS; and for amplitude:  $F_{2,28}=13.39$ , \*\*\*,  $P=0.0002$  and  $P=0.0005$  for PACAP vs. control and PBS (Tukey's multiple comparison).
- b.** Injection locations mapped onto ventral brainstem cutouts from images of parasagittal sections at two levels (1.2 and 1.32 mm lateral, from Figs. 111 and 112 of <sup>29</sup>), color coded for effect size. The approximate location of the preBötC (*orange shaded*) is based on the area caudal to FN, rostral to LRt, and ventral to NA containing neuronal *Sst*-expression (*not shown*).
- c.** Rate histogram of inspiratory burst frequency and integrated dEMG during vehicle, DLH (40 pmol) and PACAP (0.3 pmol) injection into the ipsilateral and contralateral preBötC of an anesthetized mouse 4 weeks after on-target unilateral injection of PAC1-shRNA-expressing lentivirus (ipsilateral data reproduced from Fig. 3b, ipsilateral injection sites shown in Fig. 3d).
- d.** *Upper.* Photomicrograph from parasagittal brainstem section of the single mouse (of N=6) with an off-target injection of PAC1 shRNA lentivirus (i.e., outside the preBötC). The approximate boundary of virally-transduced cells (mCherry-expressing) outside the preBötC (*red dashed area*) and PACAP injection site in the preBötC (*green*) were mapped onto ventral brainstem cutout (from Fig. 111 of <sup>29</sup>). Parasagittal section, scale bar = 200  $\mu\text{m}$ . *Lower.* Corresponding rate histogram of inspiratory burst frequency and integrated dEMG during vehicle, DLH (40 pmol) and PACAP (0.3 pmol) injection into the ipsilateral preBötC.
- e.** Time course depicting the effect on hypoglossal nerve burst frequency (mean  $\pm$  SEM) of pressure injections of PACAP (1  $\mu\text{M}$ , 10  $\mu\text{M}$ ) into the preBötC of rhythmic brain slice preparations prepared from two age groups of neonatal mice (P0-P3, N=8 slices; P9-P10, N=7 slices).
- f.** Peak relative hypoglossal nerve burst frequency after PACAP application (1  $\mu\text{M}$  and 10  $\mu\text{M}$ ) in rhythmic brain slice preparations were not different in two age groups of neonatal mice (P0-P3, P9-P10); data from all ages were pooled for statistical analysis. \*,  $P=0.0316$ , \*\*\*\*,  $P<0.0001$  relative to baseline, by ANOVA.
- g.** Rhythmic brain slice (P0) was bathed in 5 mM  $\text{K}^+$  to reduce network excitability and the effect of pressure injection of PACAP (100 nM) on hypoglossal nerve burst activity was determined. *Inset.* Peak relative hypoglossal nerve burst frequency after 100 nM PACAP injection in slices bathed in 5 mM  $\text{K}^+$  (P0-P3, N=6).
- h.** Multiplex *in situ* hybridization for *Sst* and *PAC1* transcripts combined with ChAT immunostaining in parasagittal brainstem sections containing the preBötC from mice at the indicated embryonic and postnatal ages. Images representative of (mice:litters): e19.5 (12:3), P1 (11:3), P4 (8:3), P7 (8:3), P14 (8:3), and P120 (3). Parasagittal sections, scale bar = 100  $\mu\text{m}$ .
- i.** Multiplex *in situ* hybridization for *Sst* and either *VPAC1* (*V1pr1*, *upper*) or *VPAC2* (*V1pr2*, *lower*) transcripts combined with ChAT immunostaining in parasagittal brainstem sections containing the preBötC from mice at the indicated embryonic and postnatal ages. Note the absence of either VPAC1 or VPAC2 expression in preBötC neurons, with a

developmental increase in VPAC2 transcripts evident in ChAT-IR neurons of the nucleus ambiguus beginning around P7 and persisting into adulthood (*arrows*). Images representative of (mice:litters): e19.5 (9:3), P1 (9:3), P4 (6:3), P7 (6:3), P14 (6:3), and P120 (3) Parasagittal sections, scale bar = 100  $\mu\text{m}$ .



**Extended Data Figure 6. Localization of PAC1 shRNA lentiviral transduction sites in the preBötC and effects on CO<sub>2</sub>-stimulated breathing.**

**a,b.** *Upper:* Bilateral fluorescent images of transduction region overlaid on dark field images of parasagittal brainstem sections from mice injected with PAC1 shRNA-expressing (**a**) and control (**b**) lentivirus. Parasagittal sections, scale bars = 500  $\mu\text{m}$ . *Lower, left:* Viral transduction regions from the two images were superimposed on a schematic of the relevant brainstem region (adapted from Plate 111 of <sup>29</sup>). The preBötC region (orange shaded) was approximated based on a similar tracing of concentrated *Sst* expression (*not shown*), and by its relationship to select anatomical features. *Lower, right:* The intersection of the viral transduction region with the preBötC region was determined from each of these tracings (and from a second set of bilateral images, corresponding to Plate 112 of <sup>29</sup>), and averaged to obtain a percentage overlap with the preBötC. The effect of increasing concentrations of CO<sub>2</sub> (balance O<sub>2</sub>) on V<sub>E</sub> was measured before and 4 weeks after preBötC injection of PAC1 shRNA-expressing lentivirus, and the % reduction in CO<sub>2</sub>-stimulated breathing determined (at 8% CO<sub>2</sub>).

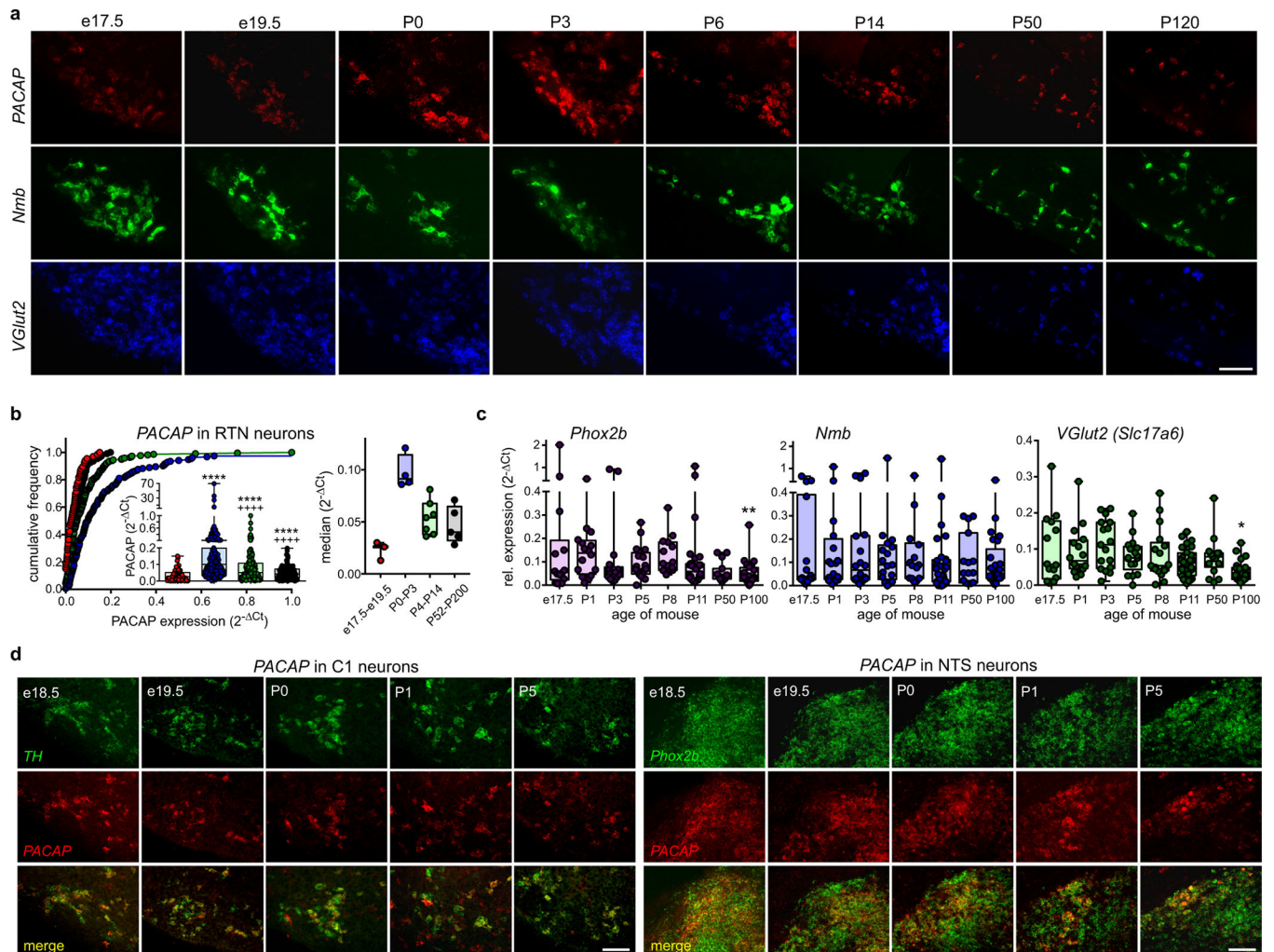
**c.** Percentage overlap of the viral transduction region with the preBötC in mice injected with control or PAC1 shRNA-expressing lentivirus (N=7 and 10). P=0.07, by Mann-Whitney test. Box-and-whisker plots in this and other panels define the median, the 25–75% ile, and the minima and maxima.

**d.** Effects of raised ambient CO<sub>2</sub> (FiCO<sub>2</sub>, 4% to 8%; balance O<sub>2</sub>) on respiratory frequency (fR, breaths/min; mean  $\pm$  SEM) and tidal volume (V<sub>T</sub>,  $\mu\text{l}$ /breath/g; mean  $\pm$  SEM) before and 4 weeks following preBötC injection with either control (N=9) or PAC1 (N=11) shRNA-expressing lentivirus. V<sub>T</sub>: F<sub>3,144</sub>=0.612, P=0.6082; fR: F<sub>3,144</sub>=7.761, P<0.0001, for

condition by 2-way ANOVA. \*,  $P < 0.05$ , PAC1 shRNA vs. initial; ++,  $P < 0.01$ , PAC1 shRNA vs. control shRNA (Tukey's multiple comparison).

**e.** CO<sub>2</sub>-evoked change in  $V_E$  in *Phox2b::GFP* mice before and 4 weeks following preBötC injection of control (N=9) or PAC1 shRNA (N=13) expressing lentivirus. \*\*,  $P = 0.0039$  by two-sided Wilcoxon matched-pairs signed rank test.

**f.** Ventilation in varied ambient O<sub>2</sub> (normoxia: FiO<sub>2</sub>, 21%; hypoxia: FiO<sub>2</sub>, 10%; hyperoxia: FiO<sub>2</sub>, 100%; median, 25–75%ile with minima and maxima) from mice before and 4 weeks following RTN injection with either control (N=9) or PACAP (N=13) shRNA-expressing lentivirus.  $F_{3,108} = 1.204$ ,  $P = 0.3120$ , for treatment by 2-way ANOVA.



**Extended Data Figure 7. Developmental expression of PACAP and GAPDH in RTN neurons.**

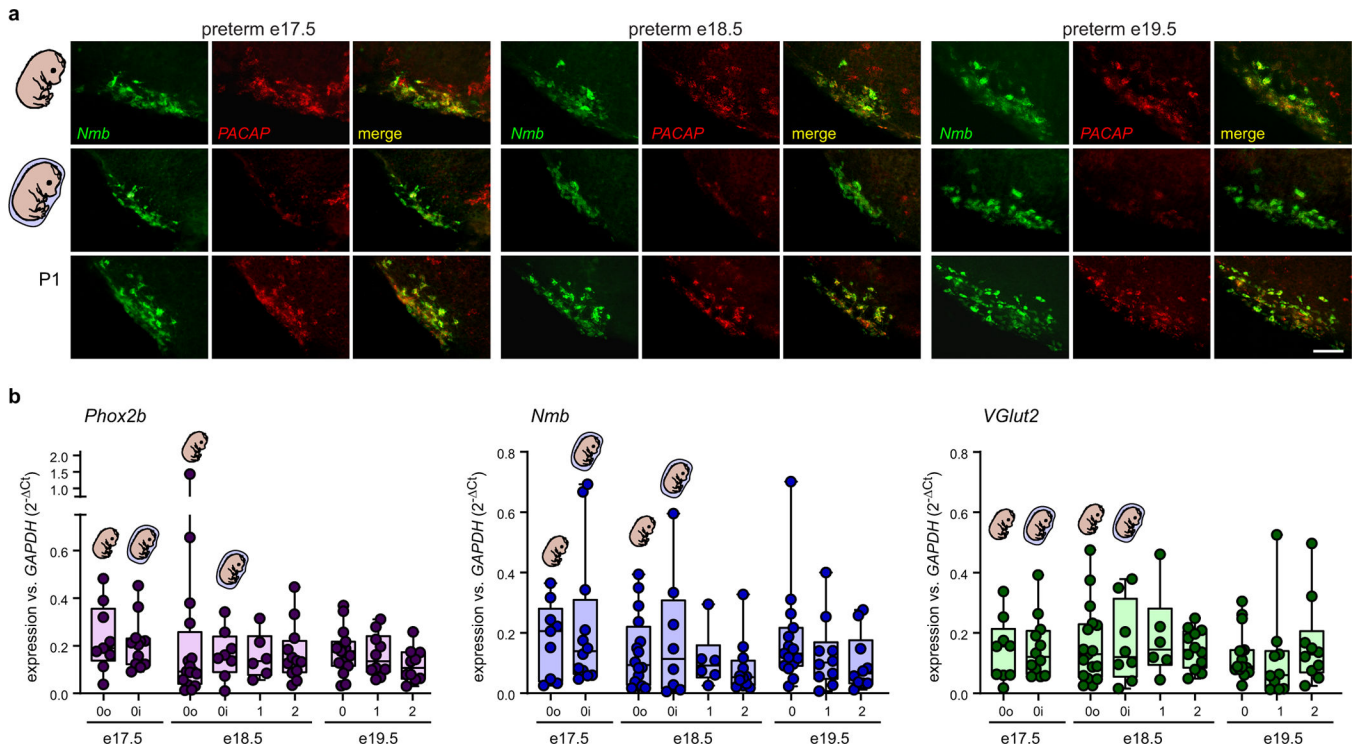
**a.** Expression of *PACAP*, *Nmb* and *VGlut2* in RTN neurons assessed by multiplex *in situ* hybridization from RTN neurons at the indicated postnatal ages. Images representative of (mice:litters): e17.5 (17:3), e19.5 (18:3), P0 (12:3), P3 (10:3), P6 (9:3), P14 (9:3), P50 (5), and P120 (4). Coronal sections, scale bar = 100  $\mu$ m.

**b.** *Left:* Cumulative probability distribution for individual PACAP expression values ( $2^{-\Delta C_t}$ , relative to GAPDH) from single cell qRT-PCR of RTN neurons at four different embryonic

and postnatal ages (cells:mice): e17.5-e19.5 (97:20); P0-P3 (150:20); P4-P14 (218:24); P52-P200 (114:14). *Inset*: Individual cell *PACAP* expression levels within each group, relative to *GAPDH* ( $2^{-\Delta C_t}$ ). Box-and-whisker plots in this and other panels define the median, the 25–75%ile, and the minima and maxima. \*\*\*\*,  $P < 0.0001$  vs. e17.5-e19.5, +++,  $P < 0.0001$  vs. P0-P3, by Kruskal–Wallis one-way ANOVA with Dunn’s multiple comparisons test. *Right*: Grouped box plot of median values for each of the embryonic and postnatal ages. (From raw data presented in Fig. 4b).

**c.** Expression of *Phox2b*, *Nmb*, and *VGlut2* assessed by multiplex sc-qPCR from RTN neurons harvested from brainstem slices at the indicated postnatal ages (cells:mice): e17.5 (14:6); P1 (16:3); P3 (18:3); P5 (17:2); P8 (14:2); P11 (29:3); P50 (15:2); P100 (25:3). \*,  $P = 0.0176$ , \*\*,  $P = 0.0026$ , by Kruskal–Wallis ANOVA with multiple Dunn’s post-hoc comparisons to P1.

**d.** Multiplex *in situ* hybridization at the indicated postnatal ages for *PACAP* expression in *TH*-expressing neurons in the caudal C1 region (–6.9 mm, relative to Bregma) and in *Phox2b*-expressing NTS neurons (–7.1 mm, relative to Bregma). Images representative of (mice:litters): e18.5 (12:3), e19.5 (12:3), P0 (10:3), P1 (8:3), and P5 (8:3). Coronal sections, scale bar = 100  $\mu\text{m}$ .

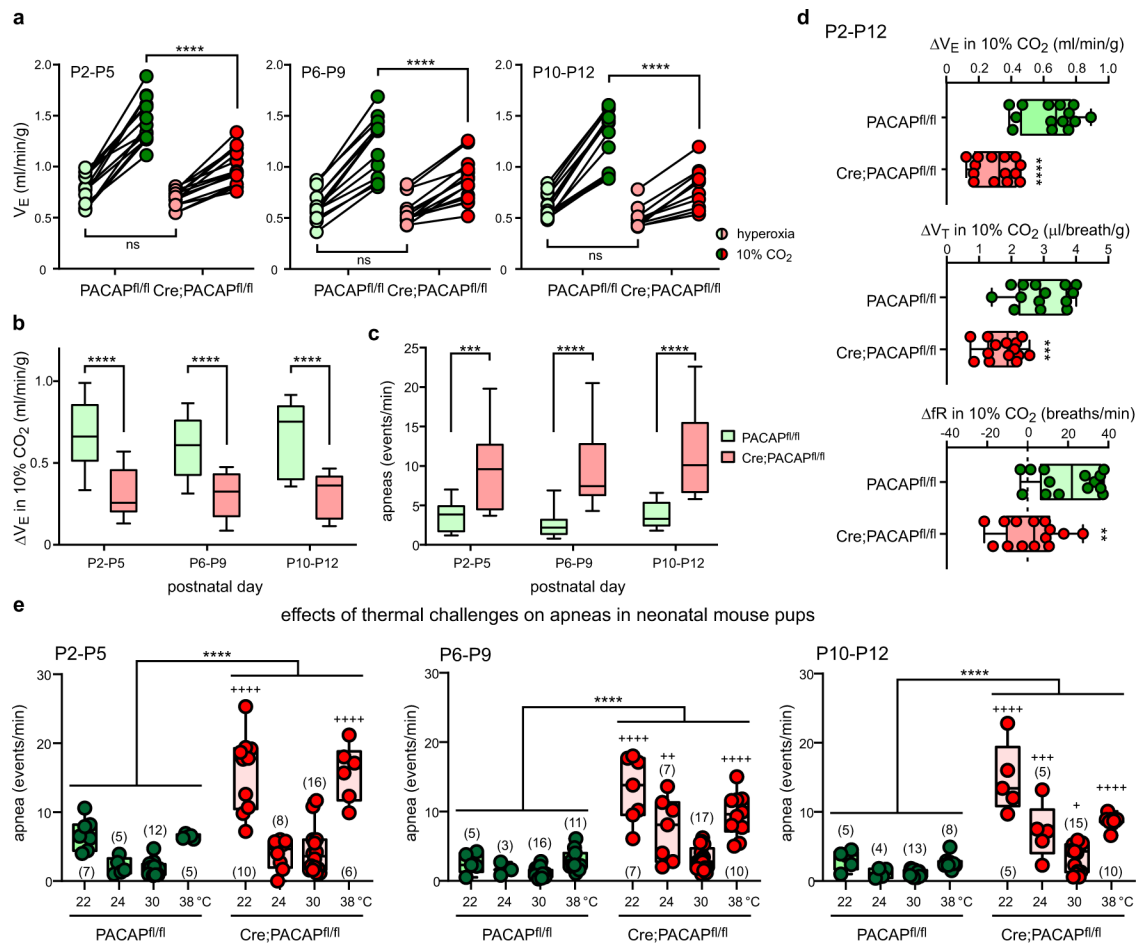


**Extended Data Figure 8. PACAP expression in *Nmb*-expressing RTN neurons from pre-term mice.**

**a.** Multiplex *in situ* hybridization for *PACAP* and *Nmb* in RTN neurons from pre-term mice born at e17.5, e18.5, and e19.5. Newborn pups were extracted from the amniotic sac by the dam (*upper row*), retained in the amniotic sac until transcardial perfusion (*middle row*), or obtained after one day of postnatal life (*lower row, P1*). The data are representative of

(mice:litters): e17.5, P0o (12:3), P0i (6:3), P1 (6:3); e18.5, P0o (12:3), P0i (5:3), P1 (6:3); e19.5, P0o (13:3), P0i (4:3), P1 (6:3). Coronal sections, scale bar = 100  $\mu$ m.

**b.** Expression of *Phox2b*, *Nmb*, and *VGlut2* assessed by multiplex sc-qPCR from RTN neurons harvested from brainstem slices of preterm mouse pups (e17.5-e19.5) at the indicated postnatal days (P0-P2); at birth (P0), some pups were taken en caul (in the amniotic sac; P0i) or after maternal extraction from the amniotic sac (P0o). (n:N values as in Fig. 4e). Box-and-whisker plots define the median, the 25–75% ile, and the minima and maxima.



**Extended Data Figure 9. CO<sub>2</sub>-stimulated breathing and apnea incidence in conditional PACAP knockout mice across the early postnatal period and during thermal stress.**

**a.** Ventilation in hyperoxia (60% O<sub>2</sub>, balance N<sub>2</sub>) and in hyperoxic hypercapnia (10% CO<sub>2</sub>, 60% O<sub>2</sub>, balance N<sub>2</sub>) in *Phox2b::Cre;PACAP<sup>fl/fl</sup>* mice and Cre-negative, *PACAP<sup>fl/fl</sup>* control littermates (n=14 pups each, from 3 litters) at different early postnatal ages (P2-P5, P6-P9, P10-P12). \*\*\*\*, P<0.0001, for genotype by 2-way RM ANOVA (Sidak's multiple comparison).

**b.** Summary data of the CO<sub>2</sub>-induced change in V<sub>E</sub> at the indicated early postnatal ages for *Phox2b::Cre;PACAP<sup>fl/fl</sup>* mice and Cre-negative, *PACAP<sup>fl/fl</sup>* control littermates (P2-P5, N=14 each; P6-P9, N=14 each; P10-P12, N=11 & 13). Box-and-whisker plots in this and other panels define the median, the 25–75% ile, and the minima and maxima. F<sub>1,74</sub>=78.42,

$P < 0.0001$ , for genotype by 2-way ANOVA. \*\*\*\*,  $P < 0.0001$  genotype effect for age group (Sidak's multiple comparison).

**c.** Summary data of apnea incidence in Phox2b::Cre;PACAP<sup>fl/fl</sup> mice and Cre-negative, PACAP<sup>fl/fl</sup> control littermates at different early postnatal ages (P2-P5, N=13 & 14; P6-P9, N=14 each; P10-P12, N=13 each).  $F_{1,75}=69.13$ ,  $P < 0.0001$ , for genotype by 2-way ANOVA. \*\*\*,  $P=0.0002$ , \*\*\*\*,  $P < 0.0001$  genotype effect for age group (Sidak's multiple comparison).

**d.** Summary data for the CO<sub>2</sub>-induced change in V<sub>E</sub> (ml/min/g), V<sub>T</sub> (μl/breath/g), and fR (breaths/min) in Phox2b::Cre;PACAP<sup>fl/fl</sup> mice and Cre-negative, PACAP<sup>fl/fl</sup> control littermates (n=14 pups each, from 3 litters); data from individual mice at different ages (P2-P5, P6-P9, P10-P12) were averaged, and treated as a single data point for analysis between genotypes. \*\*\*\*,  $P < 0.0001$ , \*\*\*,  $P=0.0002$ , \*\*,  $P=0.0032$  (by unpaired t-test).

**e.** Summary data of apnea incidence in Phox2b::Cre;PACAP<sup>fl/fl</sup> mice and Cre-negative, PACAP<sup>fl/fl</sup> control littermates at different ages (P2-P5, P6-P9, P10-P12); mice were studied in normoxia at the indicated ambient temperatures (N, number of mice for each age and condition). \*\*\*\*,  $P < 0.0001$ , for genotype effect by 2-way ANOVA; +,  $P=0.0143$ , ++,  $P=0.0059$ , +++,  $P=0.0002$ , +++++,  $P < 0.0001$ , comparing Cre- vs. Cre+ at the indicated ambient temperatures (Sidak's multiple comparison).

## Supplementary Material

Refer to Web version on PubMed Central for supplementary material.

## Acknowledgements

This work was supported by NIH research grants: R01 HL108609 (DAB), R01 HL074011 (PGG), R01 DK096010 and R01 DK075632 (BBL), and K08 DK118201 (RAR); by grants from CCHS Family Foundation (DAB), CIHR (159551, GDF), and WCHRI (GDF & RJR); and by T32 HL007374 (RAR) and a Harrison Undergraduate Research Award (AS). The authors thank Christopher Bayliss, Yu-Hsin Chiu, Elizabeth Gonye, Adishesh Narahari (Bayliss lab) for technical support and suggestions; Drs. Stephen Abbott and George Souza for suggestions regarding dEMG and plethysmography analysis; Dr. Jens Hannibal for antibody used to evaluate PACAP re-expression in HEK293T cells, and Dr. Kodi S. Ravichandran for helpful edits of the manuscript.

## REFERENCES

1. Del Negro CA, Funk GD & Feldman JL Breathing matters. *Nat Rev Neurosci* 19, 351–367, doi:10.1038/s41583-018-0003-6 (2018). [PubMed: 29740175]
2. Guyenet PG et al. The Retrotrapezoid Nucleus: Central Chemoreceptor and Regulator of Breathing Automaticity. *Trends Neurosci* 42, 807–824, doi:10.1016/j.tins.2019.09.002 (2019). [PubMed: 31635852]
3. Ruffault PL et al. The retrotrapezoid nucleus neurons expressing Atoh1 and Phox2b are essential for the respiratory response to CO(2). *Elife* 4, doi:10.7554/eLife.07051 (2015).
4. Holloway BB, Viar KE, Stornetta RL & Guyenet PG The retrotrapezoid nucleus stimulates breathing by releasing glutamate in adult conscious mice. *The European journal of neuroscience* 42, 2271–2282, doi:10.1111/ejn.12996 (2015). [PubMed: 26096172]
5. Weese-Mayer DE et al. An official ATS clinical policy statement: Congenital central hypoventilation syndrome: genetic basis, diagnosis, and management. *Am J Respir Crit Care Med* 181, 626–644, doi:10.1164/rccm.200807-1069ST (2010). [PubMed: 20208042]
6. Shi Y et al. Neuromedin B Expression Defines the Mouse Retrotrapezoid Nucleus. *The Journal of neuroscience : the official journal of the Society for Neuroscience* 37, 11744–11757, doi:10.1523/JNEUROSCI.2055-17.2017 (2017). [PubMed: 29066557]

7. Cummings KJ et al. Sudden infant death syndrome (SIDS) in African Americans: polymorphisms in the gene encoding the stress peptide pituitary adenylate cyclase-activating polypeptide (PACAP). *Acta Paediatr* 98, 482–489, doi:10.1111/j.1651-2227.2008.01131.x (2009). [PubMed: 19120039]
8. Cummings KJ, Pendlebury JD, Sherwood NM & Wilson RJ Sudden neonatal death in PACAP-deficient mice is associated with reduced respiratory chemoresponse and susceptibility to apnoea. *The Journal of physiology* 555, 15–26, doi:10.1113/jphysiol.2003.052514 (2004). [PubMed: 14608012]
9. Gray SL, Cummings KJ, Jirik FR & Sherwood NM Targeted disruption of the pituitary adenylate cyclase-activating polypeptide gene results in early postnatal death associated with dysfunction of lipid and carbohydrate metabolism. *Mol Endocrinol* 15, 1739–1747, doi:10.1210/mend.15.10.0705 (2001). [PubMed: 11579206]
10. Ross RA et al. PACAP neurons in the ventral premammillary nucleus regulate reproductive function in the female mouse. *Elife* 7, doi:10.7554/eLife.35960 (2018).
11. Rossi J et al. Melanocortin-4 receptors expressed by cholinergic neurons regulate energy balance and glucose homeostasis. *Cell Metab* 13, 195–204, doi:10.1016/j.cmet.2011.01.010 (2011). [PubMed: 21284986]
12. Shi Y et al. Nalc1n Is a “Leak” Sodium Channel That Regulates Excitability of Brainstem Chemosensory Neurons and Breathing. *The Journal of neuroscience : the official journal of the Society for Neuroscience* 36, 8174–8187, doi:10.1523/JNEUROSCI.1096-16.2016 (2016). [PubMed: 27488637]
13. Hwang DY, Carlezon WA Jr., Isacson O & Kim KS A high-efficiency synthetic promoter that drives transgene expression selectively in noradrenergic neurons. *Hum Gene Ther* 12, 1731–1740, doi:10.1089/104303401750476230 (2001). [PubMed: 11560767]
14. Kumar NN et al. PHYSIOLOGY. Regulation of breathing by CO<sub>2</sub> requires the proton-activated receptor GPR4 in retrotrapezoid nucleus neurons. *Science* 348, 1255–1260, doi:10.1126/science.aaa0922 (2015). [PubMed: 26068853]
15. Stornetta RL et al. A group of glutamatergic interneurons expressing high levels of both neurokinin-1 receptors and somatostatin identifies the region of the pre-Botzinger complex. *J Comp Neurol* 455, 499–512, doi:10.1002/cne.10504 (2003). [PubMed: 12508323]
16. Baertsch NA, Baertsch HC & Ramirez JM The interdependence of excitation and inhibition for the control of dynamic breathing rhythms. *Nat Commun* 9, 843, doi:10.1038/s41467-018-03223-x (2018). [PubMed: 29483589]
17. Harmar AJ et al. Pharmacology and functions of receptors for vasoactive intestinal peptide and pituitary adenylate cyclase-activating polypeptide: IUPHAR review 1. *British journal of pharmacology* 166, 4–17, doi:10.1111/j.1476-5381.2012.01871.x (2012). [PubMed: 22289055]
18. Arata S, Nakamachi T, Onimaru H, Hashimoto H & Shioda S Impaired response to hypoxia in the respiratory center is a major cause of neonatal death of the PACAP-knockout mouse. *The European journal of neuroscience* 37, 407–416, doi:10.1111/ejn.12054 (2013). [PubMed: 23136967]
19. Dudley DJ, Branch DW, Edwin SS & Mitchell MD Induction of preterm birth in mice by RU486. *Biol Reprod* 55, 992–995, doi:10.1095/biolreprod55.5.992 (1996). [PubMed: 8902208]
20. Mortola JP Influence of temperature on metabolism and breathing during mammalian ontogenesis. *Respir Physiol Neurobiol* 149, 155–164, doi:10.1016/j.resp.2005.01.012 (2005). [PubMed: 16126013]
21. Cummings KJ, Willie C & Wilson RJ Pituitary adenylate cyclase-activating polypeptide maintains neonatal breathing but not metabolism during mild reductions in ambient temperature. *American journal of physiology. Regulatory, integrative and comparative physiology* 294, R956–965, doi:10.1152/ajpregu.00637.2007 (2008).
22. Sawczenko A & Fleming PJ Thermal stress, sleeping position, and the sudden infant death syndrome. *Sleep* 19, S267–270 (1996). [PubMed: 9085528]
23. Darnall RA The role of CO<sub>2</sub> and central chemoreception in the control of breathing in the fetus and the neonate. *Respir Physiol Neurobiol* 173, 201–212, doi:10.1016/j.resp.2010.04.009 (2010). [PubMed: 20399912]

24. Willinger M, James LS & Catz C Defining the sudden infant death syndrome (SIDS): deliberations of an expert panel convened by the National Institute of Child Health and Human Development. *Pediatr Pathol* 11, 677–684, doi:10.3109/15513819109065465 (1991). [PubMed: 1745639]
25. Goldstein RD, Kinney HC & Willinger M Sudden Unexpected Death in Fetal Life Through Early Childhood. *Pediatrics* 137, doi:10.1542/peds.2015-4661 (2016). [PubMed: 27543009]
26. Filiano JJ & Kinney HC A perspective on neuropathologic findings in victims of the sudden infant death syndrome: the triple-risk model. *Biol Neonate* 65, 194–197, doi:10.1159/000244052 (1994). [PubMed: 8038282]
27. Barrett KT et al. Analysis of PAC1 receptor gene variants in Caucasian and African American infants dying of sudden infant death syndrome. *Acta Paediatr* 102, e546–552, doi:10.1111/apa.12405 (2013). [PubMed: 23981011]
28. Huang J, Waters KA & Machaalani R Pituitary adenylate cyclase activating polypeptide (PACAP) and its receptor 1 (PAC1) in the human infant brain and changes in the Sudden Infant Death Syndrome (SIDS). *Neurobiology of disease* 103, 70–77, doi:10.1016/j.nbd.2017.04.002 (2017). [PubMed: 28392470]
29. Paxinos G & Franklin KBJ *The mouse brain in stereotaxic coordinates Compact 2nd edn*, (Elsevier Academic Press, 2004).
30. Lazarenko RM et al. Acid sensitivity and ultrastructure of the retrotrapezoid nucleus in Phox2b-EGFP transgenic mice. *J Comp Neurol* 517, 69–86, doi:10.1002/cne.22136 (2009). [PubMed: 19711410]
31. Ting JT, Daigle TL, Chen Q & Feng G Acute brain slice methods for adult and aging animals: application of targeted patch clamp analysis and optogenetics. *Methods Mol Biol* 1183, 221–242, doi:10.1007/978-1-4939-1096-0\_14 (2014). [PubMed: 25023312]
32. Liss B Improved quantitative real-time RT-PCR for expression profiling of individual cells. *Nucleic Acids Res* 30, e89, doi:10.1093/nar/gnf088 (2002). [PubMed: 12202777]
33. Pfaffl MW A new mathematical model for relative quantification in real-time RT-PCR. *Nucleic Acids Res* 29, e45, doi:10.1093/nar/29.9.e45 (2001). [PubMed: 11328886]
34. Wiznerowicz M & Trono D Conditional suppression of cellular genes: lentivirus vector-mediated drug-inducible RNA interference. *J Virol* 77, 8957–8961, doi:10.1128/jvi.77.16.8957-8951.2003 (2003). [PubMed: 12885912]
35. Mortola JP Breathing pattern in newborns. *J Appl Physiol Respir Environ Exerc Physiol* 56, 1533–1540, doi:10.1152/jappl.1984.56.6.1533 (1984). [PubMed: 6735812]
36. Ramirez SC et al. Perinatal Breathing Patterns and Survival in Mice Born Prematurely and at Term. *Frontiers in Physiology* 10, doi:10.3389/fphys.2019.01113 (2019). [PubMed: 30740057]
37. Pepper DR, Landauer RC & Kumar P Postnatal development of CO<sub>2</sub>-O<sub>2</sub> interaction in the rat carotid body in vitro. *The Journal of physiology* 485 (Pt 2), 531–541, doi:10.1113/jphysiol.1995.sp020749 (1995). [PubMed: 7666372]
38. Basting TM et al. Hypoxia silences retrotrapezoid nucleus respiratory chemoreceptors via alkalosis. *The Journal of neuroscience : the official journal of the Society for Neuroscience* 35, 527–543, doi:10.1523/JNEUROSCI.2923-14.2015 (2015). [PubMed: 25589748]
39. Depuy SD, Kanbar R, Coates MB, Stornetta RL & Guyenet PG Control of breathing by raphe obscurus serotonergic neurons in mice. *The Journal of neuroscience : the official journal of the Society for Neuroscience* 31, 1981–1990, doi:10.1523/JNEUROSCI.4639-10.2011 (2011). [PubMed: 21307236]
40. Smith JC, Ellenberger HH, Ballanyi K, Richter DW & Feldman JL Pre-Botzinger complex: a brainstem region that may generate respiratory rhythm in mammals. *Science* 254, 726–729, doi:10.1126/science.1683005 (1991). [PubMed: 1683005]
41. Funk GD, Smith JC & Feldman JL Generation and transmission of respiratory oscillations in medullary slices: role of excitatory amino acids. *J Neurophysiol* 70, 1497–1515, doi:10.1152/jn.1993.70.4.1497 (1993). [PubMed: 8283211]
42. Ruangkittisakul A et al. High sensitivity to neuromodulator-activated signaling pathways at physiological [K<sup>+</sup>] of confocally imaged respiratory center neurons in on-line-calibrated newborn rat brainstem slices. *The Journal of neuroscience : the official journal of the Society for*

Neuroscience 26, 11870–11880, doi:10.1523/JNEUROSCI.3357-06.2006 (2006). [PubMed: 17108160]

43. Lorier AR et al. P2Y1 receptor modulation of the pre-Botzinger complex inspiratory rhythm generating network in vitro. *The Journal of neuroscience : the official journal of the Society for Neuroscience* 27, 993–1005, doi:10.1523/JNEUROSCI.3948-06.2007 (2007). [PubMed: 17267553]

Author Manuscript

Author Manuscript

Author Manuscript

Author Manuscript

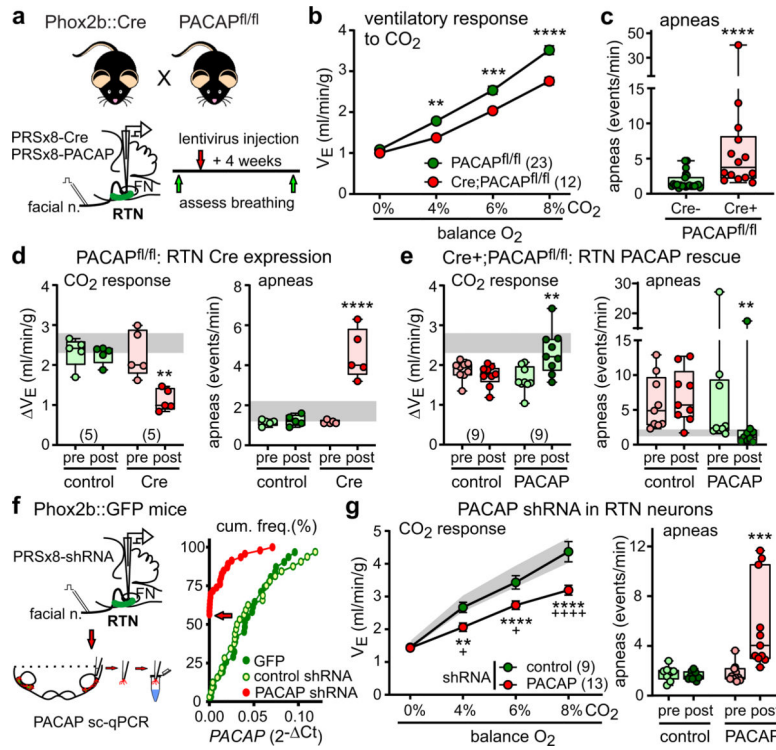


**Figure 1. Breathing is suppressed by PACAP deletion in RTN neurons.**

**a.** Phox2b::Cre and PACAP<sup>fl/fl</sup> mice were crossed to delete PACAP from Phox2b-expressing RTN neurons and PRSx8 promoter-driven lentivirus constructs were injected into mouse RTN. FN, facial motor nucleus.

**b.** Ventilatory response to elevated CO<sub>2</sub> (mean ± SEM) in Phox2b::Cre;PACAP<sup>fl/fl</sup> (N=12) and PACAP<sup>fl/fl</sup> mice (N=23).  $F_{1,132}=51.47$ ,  $P<0.0001$ , for genotype by 2-way ANOVA. \*\*,  $P=0.004$ , \*\*\*,  $P=0.0003$ , \*\*\*\*,  $P<0.0001$  (Tukey's multiple comparison).

**c.** Apnea frequency in Phox2b::Cre;PACAP<sup>fl/fl</sup> (N=14) and Cre-negative PACAP<sup>fl/fl</sup> mice (N=23). \*\*,  $P<0.0001$ , by two-sided Mann-Whitney t-test. (Box-and-whisker plots: median, 25–75%ile, minima and maxima).

**d,e.** CO<sub>2</sub>-evoked change in V<sub>E</sub> (*left*) and apnea frequency (*right*) before and 4 weeks after RTN injection of control (mCherry) or PACAP-mCherry lentivirus in Phox2b::Cre;PACAP<sup>fl/fl</sup> mice (**d**, N=9 each), and control or Cre-mCherry lentivirus in PACAP<sup>fl/fl</sup> mice (**e**, N=5 each). V<sub>E</sub>:  $F_{3,16}=11.39$ ,  $P=0.0003$ ; apnea:  $F_{3,16}=34.3$ , both  $P<0.0001$  by ANOVA; \*\*,  $P=0.012$  and \*\*\*\*,  $P<0.0001$  Cre-mCherry vs. control or pre-injection (Tukey's multiple comparison). \*\*,  $P=0.0078$  (V<sub>E</sub>) and  $P=0.0039$  (apnea), pre vs. post-PACAP by two-sided Wilcoxon matched-pairs signed rank test. Shaded regions depict 95% confidence intervals (CI) for Cre-negative PACAP<sup>fl/fl</sup> mice.

**f.** Injection of shRNA-expressing lentivirus in RTN of Phox2b::GFP mice. Cumulative frequency distribution of PACAP expression determined by qRT-PCR of individual GFP-expressing RTN neurons from uninjected Phox2b::GFP mice (GFP; 31 neurons:5 mice), or mice transduced with control (32:6) or PACAP shRNA (46:7); arrow indicates % of cells with undetectable PACAP expression. \*\*\*\*,  $P<0.0001$  vs. GFP and control, by Kruskal–Wallis one-way ANOVA and Dunn's test).

**g.** Ventilatory response to CO<sub>2</sub> (*left*; mean ± SEM) and apnea frequency (*right*) from mice before and 4 weeks following RTN injection with either control or PACAP shRNA-expressing lentivirus (N=9 and 13). CO<sub>2</sub> response: 95% CI from all mice prior to virus injection; F<sub>2,164</sub>=26.94, P<0.0001, for treatment by 2-way ANOVA. \*\*, P=0.005, \*\*\*\*, P<0.0001, PACAP vs. initial; +, P<0.05, +++++, P<0.0001, PACAP vs. control (Tukey's multiple comparison). Apnea frequency: \*\*\*, P<0.001 by two-sided Wilcoxon matched-pairs signed rank test.

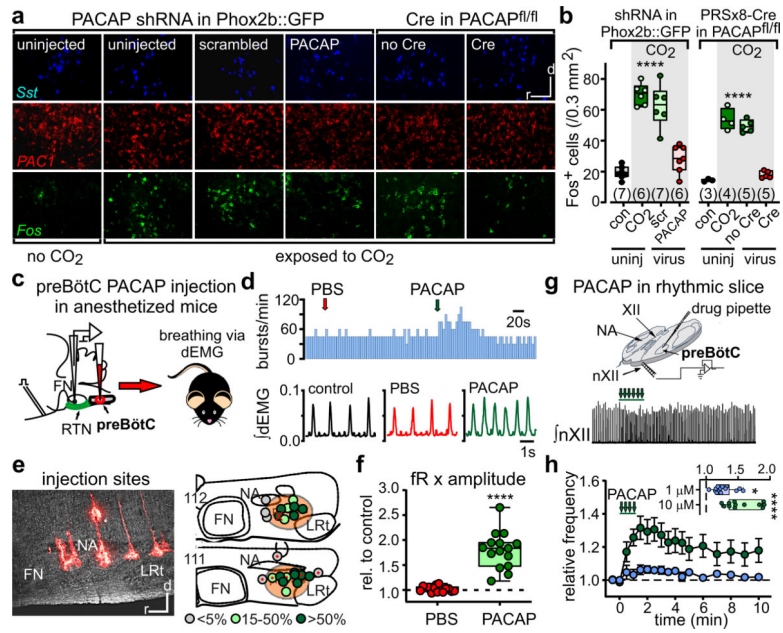


**Figure 2. CO<sub>2</sub> and PACAP activate preBötC neurons and respiratory output.**

**a,b.** Parasagittal images of CO<sub>2</sub>-induced *Fos* mRNA expression around *PAC1*-expressing cells in the preBötC (**a**) and corresponding quantification of Fos<sup>+</sup> cells under the indicated conditions (**b**, N=mice). Box-and-whisker plots: median, 25–75%ile, minima and maxima. ANOVA for Phox2b::GFP mice:  $F_{3,22}=50.79$ ; for PACAP<sup>fl/fl</sup> mice:  $F_{3,13}=97.68$ . \*\*\*\*,  $P<0.0001$ , vs. uninjected-CO<sub>2</sub> and control virus+CO<sub>2</sub> (Tukey's multiple comparison). Scale bar=100 μm, r=rostral, d=dorsal.

**c.** PACAP injection into the preBötC of anesthetized mice to determine effects on diaphragm EMG (dEMG).

**d.** Rate histogram of inspiratory burst frequency (*upper*) during injection of vehicle (PBS) and PACAP (0.3 pmol), with expanded view of integrated dEMG burst profiles (*below*).

**e.** Parasagittal brainstem section illustrating injection sites in the preBötC (*left*) that were mapped from N=6 mice (*right*) onto parasagittal ventral brainstem cutouts<sup>29</sup> (1.2 and 1.32 mm lateral, rostral at left, preBötC region shaded); sites color coded for effect on inspiratory neural output. X marks injection location for data in **d**; red dots mark injection sites depicted on *left*. Scale bar=200 μm. NA, nucleus ambiguus; LRt, lateral reticular nucleus.

**f.** Effects of PBS and PACAP injections in the preBötC (15 injections, 6 mice) on inspiratory neural output. Data normalized relative to control values before PBS.  $F_{2,28}=30.41$  by RM-ANOVA on absolute values; \*\*\*\*,  $P<0.0001$ , PACAP vs. PBS or control (Tukey's multiple comparison).

**g.** Rhythmic brainstem slice from neonatal mice (*upper*, P0-P10) and exemplar recording showing increased respiratory (nXII) burst frequency after unilateral microinjections of 10 μM PACAP (60 s) into the preBötC (P1; *lower*).

**h.** Time series of averaged effect on nXII burst frequency (mean ± SEM) and peak relative frequency of nXII burst (*inset*) after PACAP injection into the preBötC (1 μM, n=14; 10 μM, n=12; N=15 slices).  $F_{3,48}=12.44$  by ANOVA; \*,  $P=0.0147$ , \*\*\*\*,  $P<0.0001$  relative to baseline (with Bonferroni multiple comparison).

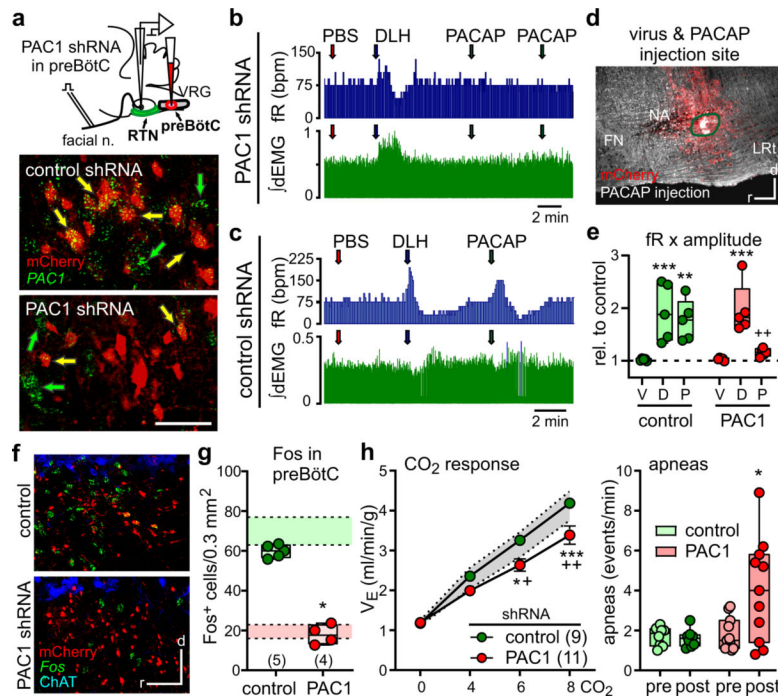


**Figure 3. PAC1 knockdown in the preBötC blocks PACAP-evoked and CO<sub>2</sub>-stimulated respiratory activation and increases apnea frequency.**

**a.** *PAC1* transcript expression in uninfected (*green arrows*) and virally-transduced (mCherry-immunoreactive; *yellow arrows*) neurons in preBötC after control (N=14) or PAC1 shRNA (N=16). Parasagittal section, scale bar=100  $\mu$ m.

**b,c.** Rate histogram of inspiratory burst frequency and integrated dEMG during injection of vehicle (PBS), DL-homocysteic acid (DLH, 40 pmol) and PACAP (0.3 pmol) in ipsilateral preBötC after viral transduction with PAC1 shRNA (**b**) or control shRNA (**c**).

**d.** Parasagittal section showing PAC1 shRNA-transduced neurons (mCherry) and PACAP injection site (*encircled*, from mouse in **b**). Representative of on-target virus and PACAP injection sites (N=5 mice each for control and PAC1 shRNA). Scale bar=200  $\mu$ m

**e.** Effects of vehicle (V), DLH (D), and PACAP (P) injections in the preBötC on inspiratory neural output in mice transduced with PAC1 shRNA or control lentivirus (N=5 each). Box-and-whisker plots: median, 25–75%ile, minima and maxima. Data normalized relative to control values before each injection.  $F_{2,24}=30.41$  by 2-way ANOVA; \*\*\*,  $P<0.0001$ , PACAP vs. PBS or control (Tukey's multiple comparison).

**f.** CO<sub>2</sub>-induced *Fos* expression in preBötC injected with lentivirus for control (N=9) or PAC1 shRNA (N=11). Immunolabeling for mCherry and ChAT denotes viral transduction and location of NA. Parasagittal section, scale bar=100  $\mu$ m.

**g.** CO<sub>2</sub>-evoked *Fos*-immunoreactive cells (mean  $\pm$  SEM) in the preBötC after control or PAC1 shRNA injection in the preBötC (N=mice). Shaded regions: 95% CI for uninjected mice  $\pm$  CO<sub>2</sub> exposure (from Fig. 2b) \*,  $P=0.0159$ , control vs. PAC1 shRNA by two-sided Mann-Whitney test.

**h.** Ventilatory response to CO<sub>2</sub> (*left*; mean  $\pm$  SEM) and apnea frequency (*right*) from mice before and 4 weeks following preBötC injection with control or PAC1 shRNA-expressing lentivirus (N=9 and 11). For CO<sub>2</sub> response: 95% CI from all mice prior to virus injection;

$F_{2,148}=9.362$ ,  $P=0.0001$ , for treatment by 2-way ANOVA. \*,  $P=0.0308$ , \*\*\*,  $P=0.0009$ , PAC1 vs. initial; +,  $P=0.0278$ ; ++,  $P=0.0029$ , PAC1 vs. control (Tukey's multiple comparison). For apnea frequency: \*,  $P=0.0127$  by two-sided Wilcoxon matched-pairs signed rank test.

Author Manuscript

Author Manuscript

Author Manuscript

Author Manuscript

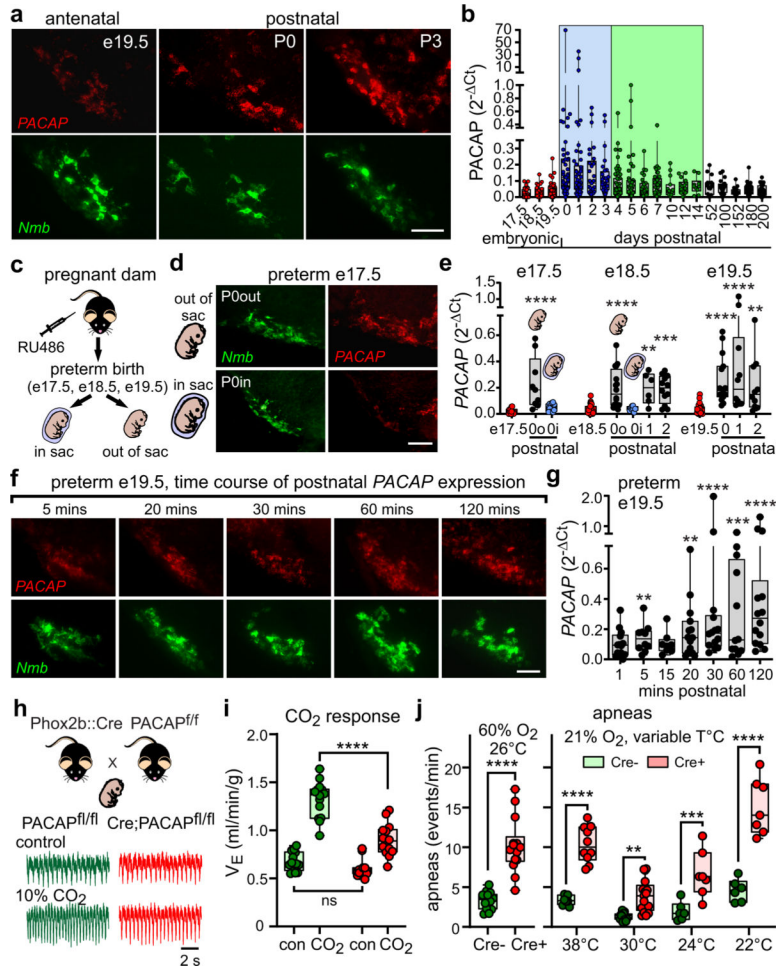


**Figure 4. Early postnatal expression and respiratory function of PACAP.**

**a.** *PACAP* transcript expression in *Nmb*-expressing RTN neurons before and after full term birth (e19.5, N=18 pups; P0, N=12; P3, N=10, from 3 litters each). Coronal section, scale bar=100  $\mu$ m.

**b.** Single cell qRT-PCR determining *PACAP* expression levels in RTN neurons harvested from *Phox2b::GFP* mice at the indicated embryonic and postnatal time points. (n=cells:N=mice): e17.5 (46:12); e18.5 (22:3); e19.5 (29:5); P0 (46:7); P1 (49:6); P2 (28:4); P3 (27:3); P4 (60:6); P5 (41:5); P6 (33:4); P7(42:4); P10 (15:2); P12 (17:2); P14 (10:1); P52 (17:2); P100 (20:3); P152 (19:2); P180 (31:5); P200 (27:2). Box-and-whisker plots: median, 25–75%ile, minima and maxima.

**c-e.** Time-mated female mice were injected with RU486 (**c**, mifepristone;150  $\mu$ g, sc) to induce preterm birth (e17.5-e19.5) and obtain pups *en caul* (in the amniotic sac; P0in) or after maternal extraction from the amniotic sac (P0out) for multiplex ISHH (**d**) or sc-qPCR (**e**). In **d** (n=mice:N=litters): P0o (12:3); P0i (6:3). In **e** (n=cells:N=mice): e17.5: 0o (9:5), 0i (12:3); e18.5: 0o (16:6), 0i (8:3), P1 (6:2), P2 (12:3); e19.5: 0o (15:5), P1 (10:3), P2 (10:2). \*\*, P<0.01, \*\*\*, P=0.0005, \*\*\*\*, P<0.0001 by Kruskal–Wallis ANOVA, with Dunn’s post-hoc comparison to corresponding embryonic time point (e17.5-e19.5, reproduced from **b**). Coronal section, scale bar=100  $\mu$ m.

**f,g.** Preterm neonatal pups (e19.5) were taken at the indicated time points following birth for multiplex ISHH (**f**; 6 mice:3 litters each) or sc-qPCR (**g**; n=cells:N=mice): 1 min, (14:2); 5 min, (10:2); 15 min (8:1); 20 min (15:2); 30 min (14:2); 60 min (12:2); 120 min (13:2). \*\*, P<0.01, \*\*\*, P=0.0005, \*\*\*\*, P<0.0001 by Kruskal–Wallis one-way ANOVA, with Dunn’s post-hoc comparison to e19.5 (from **b**). Coronal sections, scale bar=100  $\mu$ m.

**h,i.** Exemplar plethysmography traces (**h**, both P3) and summary data from neonatal Phox2b::Cre;PACAP<sup>fl/fl</sup> and PACAP<sup>fl/f</sup> pups (**i**, P2-P12; n=14 pups:N=3 litters each) under control hyperoxic conditions (60% O<sub>2</sub>) and during CO<sub>2</sub> exposure (10% CO<sub>2</sub>, 60% O<sub>2</sub>). F<sub>1,52</sub>=41.62, P<0.0001, for genotype by 2-way ANOVA. \*\*\*\*, P<0.0001 (Sidak’s multiple comparison).

**j.** *Left:* Apnea frequency determined during quiet breathing in 60% O<sub>2</sub> at 26°C. \*\*\*\*, P<0.0001, by unpaired t-test. *Right:* Separate cohorts of Cre-positive and Cre-negative PACAP<sup>fl/fl</sup> littermates tested in a thermoneutral environment (30°C) and during exposure to cold (24°C and 22°C; n = 6 & 7 for Cre- and Cre+, from 3 litters) or warm (38°C; n = 8 & 10 for Cre- and Cre+, from 4 litters). F<sub>3,67</sub>=13.73; F<sub>3,67</sub>=47.05, F<sub>1,67</sub>=163.2 for interaction, temperature and genotype, all P<0.0001 by 2-way ANOVA; \*\*, P=0.0022, \*\*\*, P=0.0002, \*\*\*\*, P<0.0001 for Cre- vs. Cre+ at the indicated temperatures (Sidak’s multiple comparison).